Lanthanide NIR Luminescence for Telecommunications, Bioanalyses and Solar Energy Conversion

ARTICLE *in* JOURNAL OF RARE EARTHS · DECEMBER 2010

Impact Factor: 1.26 · DOI: 10.1016/S1002-0721(09)60208-8

2 AUTHORS:

Jean-Claude G Bünzli
École Polytechnique Fédérale de Lausanne
483 PUBLICATIONS **16,542** CITATIONS
SEE PROFILE

Svetlana V. Eliseeva
CNRS Orleans Campus
84 PUBLICATIONS **1,437** CITATIONS
SEE PROFILE

Available online at www.sciencedirect.com
ScienceDirect
JOURNAL OF RARE EARTHS, Vol. 28, No. 6, Dec. 2010, p. 824
JOURNAL OF RARE EARTHS
www.re-journal.com/en/

Review

Lanthanide NIR luminescence for telecommunications, bioanalyses and solar energy conversion

Jean-Claude G. Bünzli[1,2], Svetlana V. Eliseeva[1,3]

(1. École Polytechnique Fédérale de Lausanne, Institute of Chemical Sciences and Engineering, BCH 1402, CH-1015 Lausanne, Switzerland; 2. WCU Professor, Korea University, Center for Next Generation Photovoltaic Systems, Jochiwon-eup, Yeongi-gun, Chungnam-do 339-700, South Korea; 3. Katholieke Universiteit Leuven, Department of Chemistry, Laboratory of Coordination Chemistry, Celestijnenlaan 200F, BUS 2404, B-3001 Leuven, Belgium)

Received 27 October 2010; revised 11 November 2010

Abstract: Present-day advanced technologies heavily rely on the exciting magnetic and spectroscopic properties of lanthanide ions. In particular, their ability to generate well-characterized and intense near-infrared (NIR) luminescence is exploited in any modern fiber-optic telecommunication network. In this feature article, we first summarize the whereabouts underlying the design of highly luminescent NIR molecular edifices and materials. We then focus on describing the main trends in three applications related to this spectral range: telecommunications, biosciences, and solar energy conversion. In telecommunications, efforts concentrate presently on getting easily processable polymer-based waveguide amplifiers. Upconversion nanophosphors emitting in the visible after NIR excitation are now ubiquitous in many bioanalyses while their application to bio-imaging is still in its early stages; however, highly sensitive NIR-NIR systems start to be at hand for both *in vitro* and *in vivo* imaging, as well as dual probes combining magnetic resonance and optical imaging. Finally, both silicon-based and dye-sensitized solar cells benefit from the downconversion and upconversion capabilities of lanthanide ions to harvest UV and NIR solar light and to boost the overall quantum efficiency of these next-generation devices.

Keywords: lanthanide; luminescence; near-infrared luminescence; telecommunications; bioanalysis; solar energy conversion; solar cell; upconversion; downconversion

1 Scope of this feature article

In recent decades, rare earths have become vital to a wealth of advanced optical materials and technologies[1] and those involving near-infrared (NIR) luminescence have stirred particular interest in view of exciting applications in telecommunications[1] and associated lasers and LED/OLED devices[2–4], as well as in bio-sciences[1,3–11], and solar energy conversion[12–16]. Erbium-doped silica optical fibers are the indispensable backbone of any modern long-range telecommunication network. Present research efforts in this field are devoted to the development of fibers and planar waveguide amplifiers made up of polymer materials in order to more easily distribute optical signals on a local scale. Low-cost and easy coupling of components by the end-user are the main sought for advantages. A good portion (ca. 650–1700 nm) of the electromagnetic spectrum, mainly belonging to the NIR range, has few interferences with biomaterials so that photons can penetrate deeply into biological samples, cells and tissues, an interesting asset for both bioanalyses and bioimaging. Additionally, IR light is less scattered than visible or UV light so that fewer losses are expected. During the past decade, the advent of upconversion nanoparticles (or nanophosphors, UCNPs) has indeed revolutionized the field of immunoassays[10,17] and these luminescent nanomaterials start to be applied with great success to bioimaging[18,19]. When it comes to sustainable energy, rare earths are one of the key components in several devices, providing for instance high coercitivity magnets[20] for windmills or electric bikes, magnetocaloric refrigerators[21,22], rechargeable lithium[23] or hydride[24] batteries, or solar cells in which rare-earth ions act as down-converters and up-converters to harvest the UV and NIR parts of the solar spectrum, respectively.

In this article, we sketch first the various strategies used for sensitizing the NIR emission of lanthanide ions before focusing on actual and potential applications. We do not intend to exhaustively cover the literature but, rather, cite the numerous recent review articles in the corresponding fields and give some general trends for each of the three chosen applications.

2 Lanthanide NIR luminescence

2.1 The NIR-emitting Ln^{III} ions

The spectral range of near-infrared (NIR) starts formally at 750 nm and extends up to 2500 nm and several trivalent visible-emitting (Ln^{III}) ions have also transitions in this range, e.g. Sm^{III} and Eu^{III}. However, the designation of lanthanide NIR-emitting ions is usually restricted to those ions mainly emitting in the NIR spectral domain. Typical transitions of

Foundation item: Project supported through grants from the Swiss National Science Foundation

Corresponding author: Jean-Claude G. Bünzli (**E-mail:** jean-claude.bunzli@epfl.ch; **Tel.**: +41-21-6939821)

DOI: 10.1016/S1002-0721(09)60208-8

the most important NIR-emitting Ln^{III} ions are shown in Fig. 1 and the characteristics of their main transitions are listed in Table 1. As far as the three selected applications are concerned, Er^{III}, which has rich photophysics with emission both

Table 1 Ground (G), main emissive (I) and final (F) states for the most important near-infrared (NIR) transitions, as well as f-f transitions participating in up- (UC) and down- (DC or QC) conversion processes

Ln	G	I	F	λ/μm or nm	E/cm^{-1}	Comment
Pr	$^3H_4$	$^1S_0$	$^1I_6$[a]	400–410	24 390–25 000	DC
		$^3P_0$	$^3H_4$	490	20 408	DC, UC
		$^1D_2$	$^3H_4$	600	16 667	DC, UC
			$^3F_4$	1.01–1.04	9 615–9 900	NIR
			$^1G_4$	1.44	6 945	NIR
		$^1G_4$	$^3H_5$	1.30–1.33	7 520–7 690	NIR, telecom line
Nd	$^4I_{9/2}$	$^2P_{3/2}$	$^4I_{9/2}$	380–390	25 640–26 315	UC
			$^4I_{11/2}$	410–420	23 810–24 390	UC
			$^4I_{13/2}$	450	22 220	UC
		$^4G_{7/2}$	$^4I_{9/2}$	520–530	18 870–19 230	UC
			$^4I_{11/2}$	580–590	16 950–17 240	UC
			$^4I_{13/2}$	650–660	15 150–15 385	UC
		$^4F_{3/2}$	$^4I_{9/2}$	870–920	10 870–11 500	NIR
			$^4I_{11/2}$	1.06–1.09	9 170–9 430	NIR
			$^4I_{13/2}$	1.32–1.39	7 195–7 575	NIR
			$^4I_{15/2}$	1.84–1.86	5 375–5 410	NIR
Sm	$^6H_{5/2}$	$^4G_{5/2}$	$^6F_{1/2}$	880	11 385	NIR
			$^6F_{7/2}$	1.02–1.04	9 615–9 800	NIR
			$^6F_{9/2}$	1.16–1.17	8 630–8 570	NIR
Eu	$^7F_0$	$^5D_0$	^7F_J (J=0–4)	570–720	13 890–17 540	DC
Gd	$^8S_{7/2}$	^6G_J	^6P_J (J=7/2–3/2)	580–650	15 380–17 240	DC
			^6I_J (J=7/2–15/2)	740–800	12 500–13 500	DC
		$^6P_{7/2}$	$^8S_{7/2}$	300–320	31 250–33 330	DC
Tb	$^7F_6$	$^5D_4$	^7F_J (J=6–0)	480–680	14 705–20 830	DC
Dy	$^6H_{15/2}$	$^6H_{9/2}$, $^6F_{11/2}$	$^6H_{15/2}$	1.28–1.34	7 575–7 810	NIR
		$^6H_{11/2}$	$^6H_{15/2}$	1.70–1.80	5 555–5 880	NIR
		$^6H_{13/2}$	$^6H_{15/2}$	2.89–3.02	3 310–3 460	NIR
Ho	$^5I_8$	$^5S_2$, $^5F_4$	$^5I_8$	530–545	18 350–18 870	UC
		$^5F_5$	$^5I_8$	650	15 385	UC
			$^5I_7$	965–990	10 100–10 360	NIR, UC
			$^5I_6$	1.48–1.51	6 630–6 760	NIR
			$^5I_5$	2.39–2.45	4 090–4 180	NIR
		$^5I_5$	$^5I_8$	910	10 990	UC
			$^5I_7$	1.63–1.68	5 965–6 120	NIR
		$^5I_6$	$^5I_8$	1.16–1.19	8 370–8 650	NIR
		$^5I_7$	$^5I_8$	1.98–2.10	4 760–5 050	NIR, laser line
Er	$^4I_{15/2}$	$^2P_{3/2}$	$^4I_{13/2}$	400	25 000	DC
			$^4I_{11/2}$	470	21 280	DC
		$^2H_{11/2}$, $^4S_{3/2}$	$^4I_{15/2}$	520–560	17 860–19 230	DC, UC
		$^4S_{3/2}$	$^4I_{9/2}$	1.70	5 880	NIR, laser line
		$^4F_{9/2}$	$^4I_{15/2}$	650–670	14 925–15 385	UC
		$^4I_{9/2}$	$^4I_{15/2}$	800	12 500	UC
		$^4I_{11/2}$	$^4I_{15/2}$	980	10 200	UC
			$^4I_{13/2}$	2.70	3 700	NIR, laser line
		$^4I_{13/2}$	$^4I_{15/2}$	1.54	6 490	NIR, telecom line
Tm	$^3H_6$	$^1D_2$	$^3F_4$	450	22 220	DC, UC
		$^1G_4$	$^3H_6$	470–475	21 050–21 280	DC, UC
			$^3F_4$	645–650	15 385–15 500	UC
		$^3H_4$	$^3H_6$	780–805	12 420–12 820	UC
			$^3H_5$	2.33	4 290	NIR
		$^3F_4$	$^3H_6$	1.75–1.90	5 260–5 710	NIR, DC
Yb	$^2F_{7/2}$	$^2F_{5/2}$	$^2F_{7/2}$	980–1.00	10 000–10 200	NIR, DC, UC

[a] Emission terminating at $^3H_4$, $^3F_4$, $^1G_4$, $^1D_2$ levels is also observed

in the visible and NIR, is the candidate of choice for telecommunications with its 1.53–1.54 μm emission line. The Pr($^1G_4 \rightarrow {}^3H_5$) transition at ≈1.3 μm and Nd($^4F_{3/2} \rightarrow {}^4I_{13/2}$) transition at ≈1.35 μm both fall within the range of another telecommunication window, but this one has not been yet fully exploited, contrary to the 1.54 μm one. Nd^{III} is an interesting ion since its absorption spectrum displays f-f transition with sizeable intensity (up to $\varepsilon \approx 10$–$12\ M^{-1}cm^{-1}$) and its main fluorescence line at 1.06 μm is the well known transition used in Nd:YAG (Yttrium Aluminum Garnet) lasers and which can be doubled to yield green emission at 532 nm, tripled to produce blue light, or quadrupled to generate UV emission at 266 nm. Several Ln^{III} ions are prone to upconversion (UC), a process in which two NIR photons are converted into one visible photon[25,26]. In most bio-applications based on UCNPs, the nanoparticles are co-doped with Er^{III} and Yb^{III}, the latter ion acting as a sensitizer[10]. Recently, Nd^{III} has been used for bio-imaging of small animals[27]. Furthermore, Yb^{III}, which emits at about 1 μm and is less sensitive to non-radiative de-activations in view of the large energy gap between the emitting ($^2F_{5/2}$) and ground ($^2F_{7/2}$) levels, is capturing much attention with respect to bio-applications[6,7,11,28]. When it comes to improving the efficiency of solar cells by upconversion, Er^{III} and Yb^{III} seem to be preferred, while downconversion (DC) or quantum-cutting (QC)[29], in which one energetic (UV or visible) photon is "cut" into two lower energy photons, requires a pair of ions: one ion can be Pr^{III}, Nd^{III}, Tb^{III}, Ho^{III}, Tm^{III}, or Er^{III}, while the other is invariably Yb^{III} which emits two photons around 1 μm, matching the band gap of silicon[13].

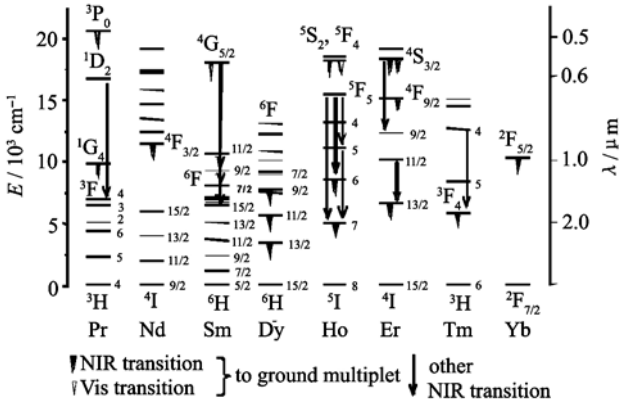

Fig. 1 Selected transitions for the most important NIR-emitting lanthanide ions. Energies are for the aquo-ions[30]. Redrawn after Ref. [11]

As will be discussed below, NIR-emitting lanthanide ions are very sensitive to radiationless de-activation through vibrations, even when embedded into inorganic matrices. Multiphonon relaxations rates have been estimated for the main NIR emission lines of Pr^{III}, Nd^{III}, Dy^{III}, Tm^{III}, and Er^{III} in function of the phonon energy[31] and this set of data should be taken into consideration when new molecules and materials are being designed.

2.2 Quantum yields and sensitization efficiency

The [Xe]$4f^n$ electronic configurations of the Ln^{III} ions generate a wealth of extremely well defined electronic levels, the spectroscopy of which is perfectly understood on the basis of crystal field and Judd-Ofelt theories[32]. The forbidden nature of electronic intraconfigurational transitions results in weak f-f electric dipole transitions, so that efficient population of the Ln^{III} excited states has to rely either on powerful excitation sources such as lasers or on a "sensitization" mechanism, referred to as "antenna effect" in which the surroundings of the metal ion harvest light and subsequently transfer energy on the Ln^{III} ion according to various processes involving several electronic states. Characteristic line-like metal-centred luminescence is then generated after fast internal conversion onto the (usually long-lived) emitting state. The entire process may be quite complex and will not be discussed here. In the case of chelates with organic ligands, triplet states often play a decisive role, as well as intra-ligand or ligand-to-metal charge transfer states[4,32].

The quantum yield of a Ln^{III}-containing inorganic or organic edifice measured upon excitation into the ligand(s), the so-called *overall* quantum yield, can be expressed by (see Fig. 2):

$$Q_L^{Ln} = \frac{I_{Ln}(E)}{I_L(A)} \tag{1}$$

The quantum yield obtained by direct excitation into the 4f level, the so-called *intrinsic* quantum yield, is given by:

$$Q_{Ln}^{Ln} = \frac{I_{Ln}(E)}{I_{Ln}(A)} = \frac{k_{rad}}{k_{rad} + \sum k_{nr}} \tag{2}$$

where k_{rad} is the radiative rate constant of the emitting level, that is in absence of any non-radiative de-activation, and one k_{nr} rate constant is associated with each non-radiative process. In a way, Q_{Ln}^{Ln} can be seen as characterizing the relative importance of radiative versus non-radiative de-activation occurring in the surroundings of the metal ion. The radiative rate constant is commonly small for Ln^{III} ions and depends on the degree of purity of the 4f states, the purest, the smallest the radiative rate constant. One way of increasing Q_{Ln}^{Ln}

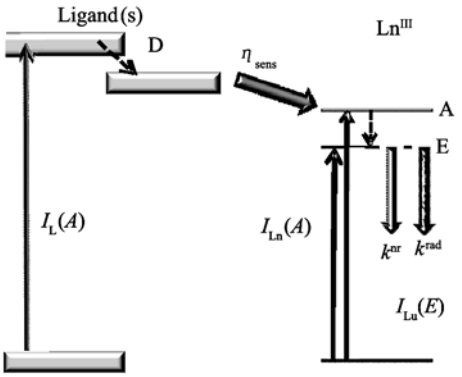

Fig. 2 Simplified scheme of the sensitization of Ln^{III} luminescence by the ligand(s) surrounding the metal ion; D is the donor state, A the acceptor state, and E the emitting state; $I(A)$ and $I(E)$ are the absorbed and emitted light intensity, respectively; k are de-activation rate constants and η_{sens} the sensitization efficiency (see text)

is therefore to design metal-ion environments having strongly polarized bonds, which leads to enhanced orbital mixing[33]. The sensitization efficiency of the metal-ion surroundings is then simply defined by:

$$\eta_{sens} = \frac{Q_L^{Ln}}{Q_{Ln}^{Ln}} \tag{3}$$

The luminescence lifetimes are the inverse of the rate constants, so that Eqs. (2) and (3) can be re-written and combined as:

$$\eta_{sens} = Q_L^{Ln} \times \frac{\tau_{rad}}{\tau_{obs}} \tag{4}$$

While Q_L^{Ln} and τ_{obs} are easy to determine experimentally, Q_{Ln}^{Ln} is often out of reach either because f-f absorptions are too weak or because they are obscured by intense ligand and/or charge-transfer (CT) transitions. In this case, τ_{rad} has to be estimated using one of the three following methods. Firstly by using Einstein's rates of spontaneous emission A from an initial state $|\Psi_J>$ to a final state $|\Psi'_{J'}>$ defined by quantum numbers S, L, J and S', L', J', respectively:

$$A(\Psi_J, \Psi'_{J'}) = k_{rad} = \frac{1}{\tau_{rad}} = \frac{64\pi^4 \tilde{\nu}_{mean}^{\ 3}}{3h(2J+1)} \left[\frac{n(n^2+2)^2}{9} D_{ED} + n^3 D_{MD} \right] \tag{5}$$

$$\tilde{\nu}_{mean} = \frac{\int \tilde{\nu} \cdot \varepsilon(\tilde{\nu})\, d\tilde{\nu}}{\int \varepsilon(\tilde{\nu})\, d\tilde{\nu}} \tag{6}$$

$\tilde{\nu}_{mean}$ is the mean energy of the transition, h is Planck's constant, and n the refractive index; D_{ED} and D_{MD} are given by the following equations:

$$D_{ED} = e^2 \cdot \sum_{\lambda=2,4,6} \Omega_\lambda \cdot \left| \left\langle \Psi_J \left\| U^\lambda \right\| \Psi'_{J'} \right\rangle \right|^2 \tag{7}$$

$$D_{MD} = \left(\frac{e \cdot h}{4 \cdot \pi \cdot m_e \cdot c} \right)^2 \cdot \left| \left\langle \Psi_J \left\| L + 2S \right\| \Psi'_{J'} \right\rangle \right|^2 \tag{8}$$

e, m_e, h, and c are the electron charge and mass, Planck's constant and the velocity of light *in vacuo*. The three phenomenological Judd-Ofelt parameters Ω_λ (in cm^2)[34] can be calculated from the f-f absorption spectrum. The squared bracketed expressions are dimensionless doubly-reduced matrix elements which are insensitive to the metal environment and which are tabulated[35]. However, except in few cases, this calculation is not trivial and large errors may occur, particularly for ions for which Judd-Ofelt theory does not apply well (e.g. Tb^{III}). Therefore, when the absorption spectrum $\varepsilon(\tilde{\nu}) = f(\tilde{\nu})$ to the emissive level is known, which may be the case when the luminescence transitions terminate onto the ground level, then:

$$k_{rad} = \frac{1}{\tau_{rad}} = 2\,303 \times \frac{8\pi c n^2 \tilde{\nu}^2 (2J+1)}{N_A (2J'+1)} \int \varepsilon(\tilde{\nu}) \mathrm{d}\tilde{\nu} \tag{9}$$

in which c is the speed of light *in vacuo* and N_A is Avogadro's number. Finally, in the case of Eu^{III}, for which the purely magnetic dipole transition $^5D_0 \rightarrow {}^7F_1$ acts as reference[36], the radiative lifetime can be determined from the quantitative (corrected for the instrumental function of the spectrometer), the refractive index and the observed lifetime, with $A_{MD,0}$=14.65 s^{-1}:

$$\frac{1}{\tau_{rad}} = A_{MD,0} \cdot n^3 \left(\frac{I_{tot}}{I_{MD}} \right) \tag{10}$$

Irrespective of the method used, the experimental measurements leading to the determination of τ_{rad} and subsequently Q_{Ln}^{Ln} and η_{sens} are not easy to conduct with the required accuracy, especially for NIR-emitting ions, so that "literature values" are often used. However, care should be exercised since τ_{rad} is dependent on both n and the composition of the inner coordination sphere. These aspects are discussed in Ref. [11] and Ref. [33].

2.3 Sensitization strategies

Several energy transfer strategies have been explored to sensitize the luminescence of NIR-emitting Ln^{III} ions: (i) transfer from an organic ligand with singlet, triplet, or intra-ligand charge-transfer CT states (ILCT) being the main donors, (ii) transfer from a d-state of a transition metal cation such as Cr^{III}, Ru^{II}, Ir^{III}, (iii) sensitization by another Ln^{III} ion, for instance Yb^{III}-to-Er^{III} transfer, or (iv) for Yb^{III} only, excitation of the $^2F_{5/2}$ state by electron transfer since $E^0(Yb^{III}/Yb^{II}) = -1.05$ V only[11]. Optimization of the energy transfer always requires (i) maximum overlap between the emission spectrum of the donor state (D) and the absorption spectrum of the acceptor Ln^{III} ion (A), (ii) adequate energy match between D and A, as well as (iii) a ligand design adapted to the principal mechanism operating the transfer of energy. Long-range through-space dipole-dipole (Förster) transfers occur between two metal ions, while shorter range through-bond exchange (Dexter) transfers are usually operating between an organic entity and the Ln^{III} ion. Recently, a long-range super-exchange mechanism has been identified in the energy transfer between d- and f-transition metal ions, which is made possible thanks to a conjugated electronic bridge[37].

2.3.1 Organic ligands

Detailed descriptions can be found in several recent reviews[4,7,11,38–40], so that we only sketch the more salient features here.

Macrocyclic ligands (Scheme 1)

Several research groups have systematically investigated a number of ligand classes. Among the first ones are porphyrinates which possess low-energy levels (14–15 000 cm^{-1}) ideally suited for transferring energy onto Yb^{III} for instance[11,39]. These ligands feature a planar substrate not completely ideal for fully saturating the Ln^{III} coordination sphere but, on the other hand, ancillary ligands can be used to fill the gaps and to tune the photophysical properties. Further adjustments are available through grafting substituents in the available R_1, R_2, and R_3 positions[38]. Metalloporphyrinates with Zn^{II} or Cu^{II} also sensitize Yb^{III} luminescence since coordination of the d-transition metals hardly modifies the energy of the donor levels[41].

The ubiquitous cyclen framework (8 donor atoms) is very

appropriate to yield highly stable and kinetically inert complexes with almost saturated coordination sphere; it lends itself to easy derivatization and dozens of variations have been proposed, featuring well adapted chromophores[39,42,43], so that not only Yb^{III} but also Nd^{III} and Er^{III} luminescence could be sensitized[42,44]. Coronands, cyclic Schiff bases and cryptands also provide versatile coordination to lanthanide ions and some of them bearing suitable derivatization were used to design NIR-luminescent complexes. To date, the best performance has been obtained in aqueous solution with benzo-azacrown ligand **1b** with which the dinuclear Yb^{III} complex displays the largest quantum yield reported for this ion in aqueous solution to date (0.53%).

Acyclic ligands (Scheme 1)

Lanthanide β-diketonates are known for more than a hundred years and have generated a wealth of developments in view of the peculiar properties of these compounds. Neutral tris complexes have coordination number equal to 6 so that at least two coordination sites remain free and can be filled by an ancillary ligand, which allows a large tuning of the photophysical properties. The volatility of β-diketonates is an asset for vapor deposition of thin films which are used in electroluminescent devices and most of them are quite luminescent because they have a short radiative lifetime (see Eq. (4)) due to highly polarized ligand-Ln bonds. Sensitization of Yb^{III} luminescence by dibenzoylmethanate (DBM) was demonstrated in 1958[45], but interest rapidly died out until the work of Meshkova et al. in the 1980s and 1990s who proposed to use β-diketonates for the analytical determination of lanthanide ions in advanced materials. This generated very systematic investigations of the effect of substituents, ancillary ligands, and symmetry on the luminescence intensity and the various contributions to non-radiative de-activation of Yb^{III} could be sorted out on the basis of careful recording of quantitative quantum yield and lifetime data and deuteration of the ligands[46]. Presently, the quest for more efficient electroluminescent materials for OLEDs still leads to the development of devices based on β-diketonates[47,48].

After the discovery of the 1.54 μm Er^{III} luminescence in [Er(**8Q**)$_3$], where **8Q** is 8-hydroxyquinolinate, in 1999 by Gillin et al.[49] and subsequently metal-centred luminescence in the corresponding [Nd(**8Q**)$_3$][50] and [Yb(**8Q**)$_3$][51] complexes, several derivatives of this chromophore[52,53], including podands[28,54,55] and macrocycles[56] have been proposed with success for the sensitization of Nd^{III}, Er^{III}, and Yb^{III}. With respect to the last ion, overall quantum yields in the range of 3.1–3.7% could be obtained with ligands **2** for solid state Na-Yb heterobinuclear samples, while they reach 1–2% in trinuclear heterobimetallic helicates[57].

The acyclic *m*-terphenyl framework derivatized with carboxylic functions provides suitable coordination ability to efficiently encapsulate lanthanide ions. It has been fitted with chromophoric dyes such as triphenylene, dansyl, coumarin, lissamine, Texas red, fluorescein, eosin, erythrosin (see H_3**3** in Scheme 1) which have low-energy triplet states allowing sizeable sensitization of Ln^{III} NIR luminescence[58].

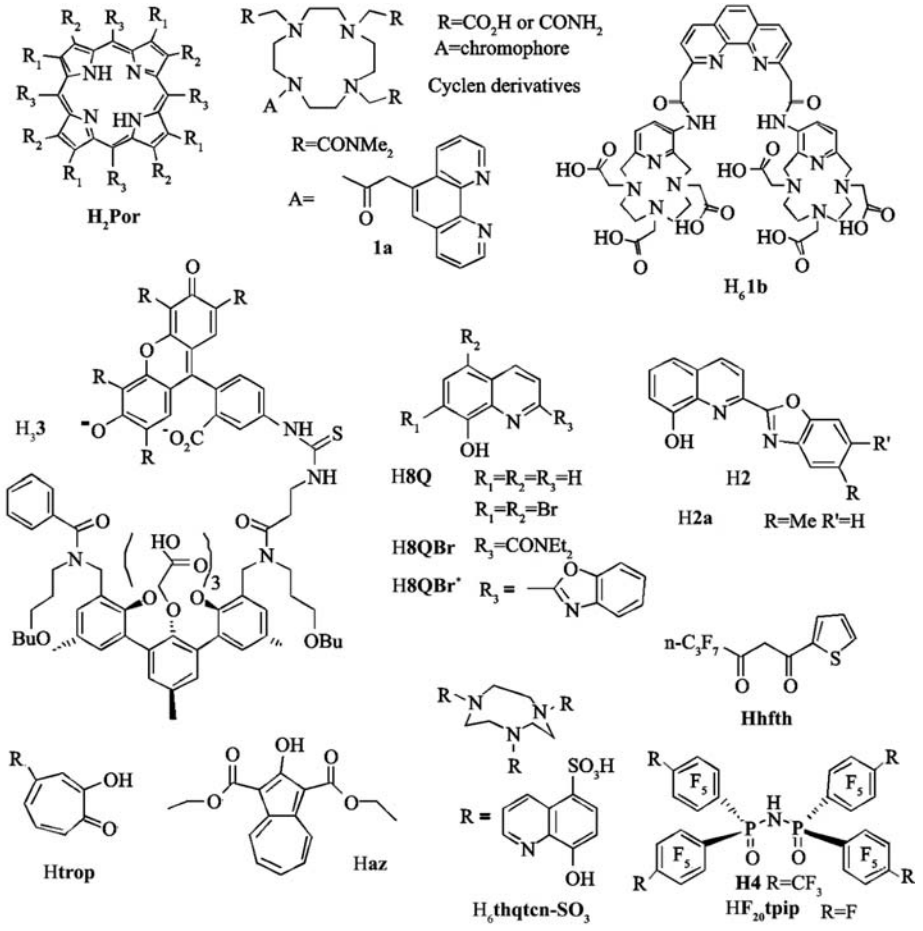

Scheme 1 Examples of ligands for the sensitization of NIR-emitting Ln^{III} ions

The obtained quantum yields remain however modest, even in deuterated methanol: ≈0.15% and ≈0.55–0.60% for Nd^{III} and Yb^{III}, respectively. The same or similar dyes have also been grafted on polyaminocarboxylate backbones.

Simpler ligands such as the Schiff base salophen, tropolonate, azulene dicarboxylate, or pyridine carboxylate molecules have been the subject of a recent review[7]. Among the corresponding chelates, the octadentate complexes $[Ln(\mathbf{trop})_4]^-$ and $[Ln(\mathbf{az})_4]^-$ display remarkable overall quantum yields, reaching 1.9% and 3.8%, respectively, in DMSO and acetonitrile for Ln=Yb[7,59,60]. Acridone-benzimidazole fused ligands have also been reported to transfer energy on Yb^{III}, but the corresponding overall quantum yields in acetonitrile are smaller, at most 0.86%[61].

Extended structures (Scheme 2)

Metal-organic frameworks (MOFs) offer the advantage of being able to encapsulate metal ions at pre-determined distance, therefore avoiding detrimental concentration quenching and, possibly enhancing through-space antenna effect by a better positioning of the chromophoric groups. They are usually obtained by easily controllable sol-gel methods, resulting in high purity and optical quality, as well as tuning of the refractive index[62,63]. Another advantage is that simple ligands such as benzenedicarboxylate ($\mathbf{bdc}^{2-}$) and benzenetricarboxylate ($\mathbf{btc}^{3-}$) lead to such inorganic-organic hybrids, avoiding lengthy synthetic work of multidentate chelating molecules. An example is given in Fig. 3 which displays the structure of $\{[Er(\mathbf{btc})(H_2O)_5]\cdot 3.5H_2O\}_\infty$ in which the ten shortest Er…Er contacts lie between 0.72 and 1.22 nm. Similar distances are obtained for $[Er_2(\mathbf{bdc})_3(H_2O)_4]_\infty$ which, upon dehydration, transforms into $[Er_2(\mathbf{bdc})_3]_\infty$ having an overall quantum yield of 0.022%, similar to the one exhibited by other Er^{III} complexes with organic ligands[64]. Other examples include $\mathbf{PVDC}^{2-}$[65,66], 3,5-pyridinedicarboxylate[67], 2,6-pyridinedicarboxylate[68], 2,5-thiophene-dicarboxylate[69], derivatized triazole[70], or multidentate chelating agents[71] as ancillary ligands. Mixtures of ligands also result in interesting extended structures[72].

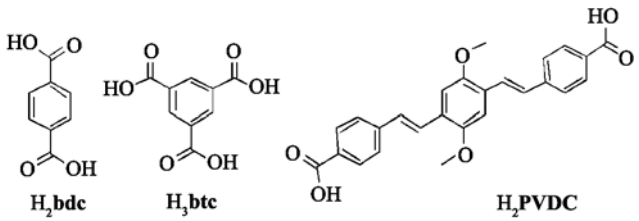

Scheme 2 Simple ancillary ligands for building coordination polymers

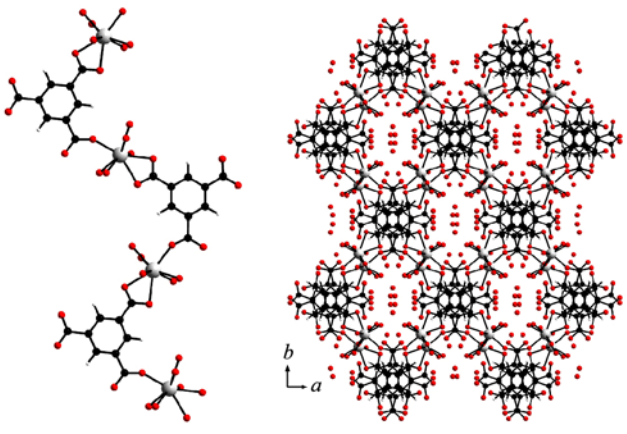

Fig. 3 Projection view of a molecular motif of $\{[Er(\mathbf{btc})(H_2O)_5]\cdot 3.5H_2O\}_\infty$ (left). Projection view along the $\vec{c}$ axis of the crystal packing (right). Reproduced with permission from Ref. [64], © Wiley VCH, 2009

In order to overcome the problem of very low Er^{III} and Nd^{III} quantum yields, these ions have been inserted into dendrimeric structures. For Nd^{III}, the light-harvesting chromophores chosen were the dansyl group[73,74], derivatized benzenetricarboxylate[75,76], naphtyl moieties[77], or a more intricate edifice in which light is transferred first onto a Ru^{II} complex which sensitizes Nd^{III} luminescence by means of the ^{3}MLCT state[78]. For Er^{III}, dansyl units are also adequate chromophores[74], as well as metalloporphyrins[79–81].

2.3.2 Sensitization of Ln^{III} luminescence by transition metal ions

Heteropolymetallic d-f complexes are well documented and relatively easy to design since the two metal ions display very different stereochemical preferences. The property of interest in these molecules is the occurrence of intense ^{1}LMCT and ^{3}MLCT states involving the d-transition metal ions, which often have suitable energy for an efficient sensitization of Ln^{III} NIR luminescence, compared for instance with the use of Cr^{III} in Nd:YAG lasers. In addition to this ion, Re^{I}, Ru^{II}, Os^{II}, Ir^{III}, Pd^{II}, and Pt^{II}, are among the most efficient d-transition metal ions for this purpose. Edifices containing these ions are presented and discussed in several review articles[3,4,11,82–87]. Some of these complexes have been designed to investigate the mechanism of energy transfer (Förster, Dexter, extended Dexter, multipolar)[37,88–90]. Another goal of investigators is to obtain systems which are reasonably luminescent in aqueous solutions for potential bio-applications[91]. Recently, ions such as Cu^{I}[92], Ag^{I}[93], and Au^{I}[94] have also been introduced in heteropolymetallic materials, while Zn^{II} is often provided as a structural building block[95,96].

2.3.3 The nightmare of C-H (and other) vibrations

Despite the wealth of new complexes and coordination polymers with organic ligands that have been synthesized during the past few years, photophysical properties remain poor for the NIR-emitting Ln^{III} ions, with maximum overall quantum yields in the ranges of 0.03–0.4% for Nd^{III}, <0.04% for Er^{III}, and 0.5–3.8% for Yb^{III} [4,7,11]. See Table 2 for a highlight of the best performances obtained during the past five years.

This situation is mainly due to the fact that researchers often concentrate solely on improving the sensitization efficiency (Eq. (4)) while not giving enough attention to enhancing Q_{Ln}^{Ln}, either by lengthening the radiative lifetime, which is difficult[33], or by minimizing radiationless de-activation by high-energy vibrations. Indeed, one of the parameters governing the value of the intrinsic quantum yield is the energy gap between the emissive level and the more energetic sub-level of the end state, ΔE_g. The smaller the gap, the easier it is to bridge with vibration overtones.

Table 2 Selected NIR-emitting systems published recently (2005–2010) and featuring sizeable luminescence sensitization by organic ligands. See Schemes 1 and 4 for chemical formulae

Complex	Sample	Q_{Ln}^{L} / %	τ/μs	Q_{Ln}^{Ln} / %	Ref.
$[Nd(SC_6F_5)_3(DME)_2]^a$	solid	n.a.	111[b]	9.3[b]	[97]
[Nd(**8QBr***)$_3$]	solid	0.33	1.82	0.67	[98]
[Nd(**az**)$_4$]$^-$	MeCN	0.45	1.85	n.a.	[60]
$[RuNd_3(\mathbf{1a})_3]^{11+}$	H_2O (pH 7.4)	0.043	0.19[b]	n.a.	[91]
$[Er(SC_6F_5)_3(DME)_2]^a$	solid	n.a.	2880	75	[99]
$[Er_{0.5}Yb_{0.5}((C_6F_5)_2POO)_3]$	nanorods	n.a.	748	5.3[c]	[100]
[Er(**8QBr**)$_3$]	solid	0.033	4.05	n.a.	[52]
[Er(**F$_{20}$tpip**)$_3$]	CD_3CN	n.a.	741	n.a.	[101]
[Er(**az**)$_4$]$^-$	MeCN	0.021	n.a	n.a.	[60]
[NaYb(**2a**)$_4$]	solid	3.6	22	3.6	[53]
[Yb(**az**)$_4$]$^-$	MeCN	3.8	24.6	n.a.	[60]
[Yb(**hfth**)$_3$phen]	toluene	1.28	14.7[d]	n.a.	[102]
[Yb(**5a**)(H**5a**)]	H_2O (pH 7.4)	0.22	1.55	n.a.	[103]

[a] DME=1,2-dimethoxyethane. [b] For $^4F_{3/2}\rightarrow{}^4I_{11/2}$ transition. [c] Recalculated from τ assuming the radiative lifetime found for Er-doped silica: 14 ms. [d] For solid state sample

This gap is around 10 000 cm^{-1} for Yb^{III}, which is relatively large and explains the reasonably large quantum yields reported for this ion, but it drops to ≈6 500 cm^{-1} for Er^{III} and even to ≈5 500 cm^{-1} for Nd^{III}. Therefore eliminating high-energy vibrations such as O–H or N–H from the inner and outer coordination sphere of these ions is not sufficient. C–H groups must also be removed, which is not easy because organic ligands usually bear a score of them and, also, because C–H quenching is operating at long distance from the metal center. This phenomenon is known for some time[46] and can be minimized by deuterating[46,104] or fluorinating the ligands[48]. The quenching ability of C–H groups (and other vibrations) is governed by two factors: the distance to the Ln ion ($1/r^6$) and the Franck-Condon overlap between the wavefunctions of the 4f excited state and the overtone of the de-activating oscillator[105].

In a seminal paper published in 2006, Gillin and collaborators have quantified the quenching of the luminescence lifetime of Er^{III} ions in the β-diketonates $[Er(hfa)_3(H_2O)_2]$ and $Cs[Er(hfa)_4]$ complexes by C–H vibrational oscillators as a function of their distance to the emitting ion. They have shown that if a dipole-dipole mechanism for energy transfer is assumed, with $1/r^6$ dependence, any hydrogen atom in a sphere of 2.0 nm from an erbium ion causes sufficient quenching to prohibit its use in telecommunications applications: 98% deuterated $Cs[Er(hfa)_4]$ displays two lifetimes, the longest one being only 106 μs. The conclusion is that deuteration is not a solution and that ligands should rather be halogenated. Indeed these authors have come up with fully fluorinated phenyliminodiphosphinate Er^{III} chelates, which display lifetimes up to 0.44 ms[106,107]. A similar conclusion had been reached by Quochi et al. after studying Er^{III} complexes with chlorinated 8-hydroxyquinolines[108] and who proposed an erbium complex with perfluorinated acetylacetonate and triphenylphosphine oxide[109]. However, full fluorination is difficult to achieve and the reported complex still displays too short a lifetime for being used as a medium for broadband NIR emission in the telecommunication window.

The quenching rate constants of C–H groups in Nd^{III} and Yb^{III} cryptates with (bpy.bpy.bpy) are reported in Fig. 4. They have been determined by measuring the lifetimes of the un-deuterated, 5 partially deuterated (D_4, D_8, D_{10}, D_{12}, D_{20}) and the fully deuterated (D_{30}) cryptates[104]. They are large, as expected, reaching 73 ms^{-1} for the equatorial H in the Nd^{III} compound. The methylene groups quench Nd^{III} luminescence ≈12 times more efficiently than Yb^{III} luminescence and this ratio falls to about 4-fold for aromatic protons for which the r_{Ln-H} distances are longer. These data illustrate quite well the energy gap law. They also prove that the vibrational quenching indeed follows the dipole-dipole mechanism proposed by Förster, as demonstrated by the perfect linearity of the plot Δk(H–D) versus $(1/r_{Ln-H})^6$ illustrated in Fig. 5 for Nd^{III}. Finally, it is noteworthy that the lifetimes for the two fully deuterated species remain short, 9.1 μs for Nd^{III} and 11 μs for Yb^{III}, pointing to still appreciable quenching by C–D and other framework vibrations.

Other energetic vibrations, e.g. C=C, C=O, or even C–O, are also inducing sizeable nonradiative deactivations. This is exemplified in the work of Brennan and collaborators who found that fluorinated phenoxide complexes $[Ln(OC_6F_5)_3(DME)_2]$ (DME is 1,2-dimethoxyethane) are less lumines-

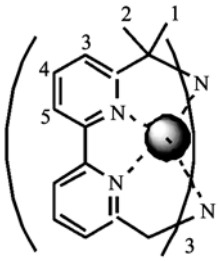

H	r_{Nd-H}	Nd	Yb	Nd/Yb
1_{eq}	3.58	73	5.7	12.8
2_{ax}	4.38	22	2.0	11.0
3	5.54	3.9	0.9	4.3
4	6.32	1.7	0.4	4.3
5	5.50	3.8	0.9	4.2

Fig. 4 Quenching rate constant differences Δk(H-D)=k(H)–k(D) in ms^{-1} for the various C-H oscillators in the [Ln(bpy.bpy.bpy)]$^{3+}$ cryptates; Nd^{III}-H distances are given in 10^{-1} nm[104]

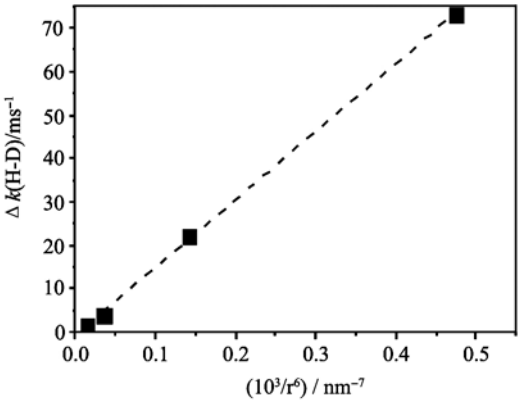

Fig. 5 Dependence of the quenching rate constant difference Δk(H-D) versus $(1/r_{Ln-H})^6$ for $[Nd(bpy.bpy.bpy)]^{3+}$. Drawn from data reported in Ref. [104]

cent than their thiolate analogues $[Ln(SC_6F_5)_3(DME)_2]$. For Ln=Nd, the intrinsic quantum yield is 2% only compared to 9% for the thiolate complex; in the case of Er^{III}, Q_{Er}^{Er} drops to 19% from 75% for the thiolate. With coordination to the softer sulfur atoms, the vibronic coupling is less efficient and the Franck-Condon factor for the relaxation process is reduced[110].

In summary, one may be somewhat pessimistic as far as the future of organic-based complexes in information and telecommunication technologies is concerned, except if inorganic-organic hybrids are considered, as described in the next section.

2.3.4 Inorganic-organic hybrid materials

Looking into the literature, one realizes that the highest intrinsic quantum yields reported for Er^{III} are for purely inorganic materials having very low phonon energies (<700 cm^{-1}). For instance, both radiative and observed lifetimes of LaF_3:Er are equal to 12.3 ms pointing to 100 % intrinsic quantum yield[111]. It is to be stressed here that the critical distance for minimizing Er-Er dipole interactions, which are real killers of erbium luminescence, is estimated to >1.5 nm, so that inorganic clusters with double cubane structures featuring Er_xS_y motifs in which Er-Er distances are on the order of 0.4 and 1.0 nm have lower intrinsic quantum yields (75–78%) and radiative lifetimes (≈3.9 ms)[111]. These two examples clearly set the challenge of designing highly efficient NIR-emitting materials and successful attempts have been made to introduce the Ln^{III} NIR-emitting ions into zeolites, as well as into other extended structures like siloxanes, di-ureasils, ureasilicates, urethanesilicates, or into nanoparticles[11]. Eliminating water is not always easy though and materials containing organic frameworks of course suffer from the drawback discussed above. On the other hand, purely inorganic materials have low absorbance and efficient antenna effects are not easy to implement. There are two ways out to this problem. The first one is to find a suitable (mainly) inorganic antenna, such as titanate[112], tungstate[113], or fluorinated iminophosphinate[106], while the second one is a combination of an inorganic core surrounded at suitable distance by an organic chromophore (Fig. 6). Selected examples are presented in the following sections.

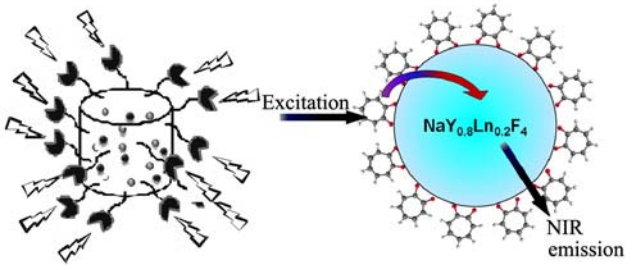

Fig. 6 Organic-inorganic hybrids in which the luminescent Ln^{III} ion is embedded into an inorganic matrix onto which organic antennae are grafted. Left: Principle; right: $NaYF_4$:Ln nanoparticles coated with a layer of tropolonate antennae; reproduced with permission from Ref. [114], © American Chemical Society 2007

3 Next-generation telecommunications devices

During the past two years, attention has mainly focused on getting better performing materials and NIR-emitting OLEDs[47], from both the photophysical and processing points of view, as well as on the design of waveguide amplifiers. Selected examples in the first category include the attempts to fluorinate organic ligands, with limited successes as seen above[48,109,115]. For instance, the intrinsic quantum yield of the Er^{III}($^4I_{13/2}$) excited level increases by one order of magnitude in going from $[Er(acac\text{-}F_6)_3OP(C_6F_5)_2]$ to $[Er(acac\text{-}F_7)_3OP(C_6F_5)_2]$, that is by fluorinating the α position of the diketonate, but remains low at 0.17% and τ_{obs} is still in the μs range (16.8 μs); in addition the emission spectrum contains appreciable intensity of the $^1S \rightarrow {}^1S_0$ transition[109]. Another endeavor involves the fluorinated iminodiphosphinate ligands H**F$_{20}$tpip** and H**4** (Scheme 1), which lead to complexes with τ_{obs} ($^4I_{13/2}$)=0.44 and 0.73 ms[106,107]. But the presence of halogenated groups on these ligands has the tendency to reduce their coordination ability.

Purely inorganic nanomaterials Ge(SiEr) have been fabricated by co-pyrolysis of germanium nanowires (NW) with SiH_4 and [Er(**tmhd**)$_3$] (Scheme 3) followed by annealing at 600–700 ºC; alternatively, NW with erbium-enriched surface, (Ge/Si/Er), can be produced from the same starting material by successive pyrolysis of the reactants followed by annealing[116]. Detailed optical data are not yet available, but the emission intensity of the surface-enriched NWs is the weakest due to the presence of erbium clusters at the surface, favoring Er-Er energy migration and quenching. Annealing temperature also affects the luminescence intensity, the higher, the better. From the reported data, both carrier-mediated and direct excitation processes determine light emission. Further development will include multilayer Er^{III}-doped SiGe NWs with greatly reduced thickness of both Si and Er, which should reduce the diffusion barrier and improve the photophysical properties[116] .

Another interesting synthetic effort is the encapsulation of a perfluorinated chromophore, decafluorobenzophenone (**DFB**, Scheme 3) into the channels of an Er^{III} exchanged zeolite L (Fig. 7). A 80-nm broad sensitized emission from

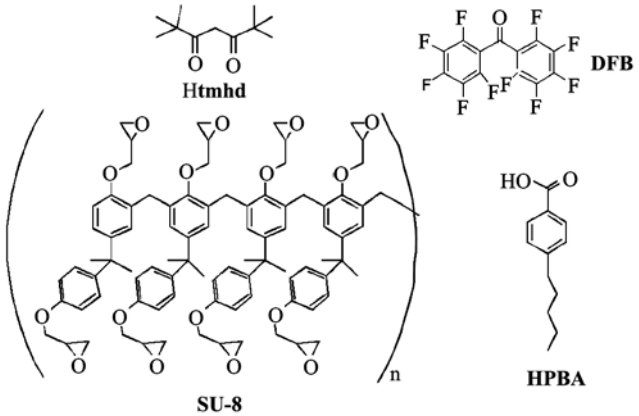

Scheme 3 Ligands and polymer for highly luminescent NIR-emitting Ln^{III} materials

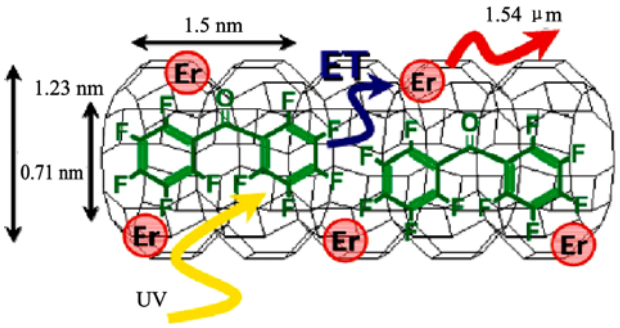

Fig. 7 Schematic drawing of the energy transfer process from the encapsulated chromophore **DFB** to Er^{III} ions embedded in zeolite L. Reproduced with permission from Ref. [117], © American Chemical Society 2010

Er^{III} is observed upon UV irradiation at 280 nm. The observed lifetime is sizeable, 0.38 ms and the corresponding intrinsic quantum yield amounts to 2.5%[117].

The fabrication of new erbium-doped waveguide amplifiers (EDWA) has relied on SU-8[118,119] (Scheme 3) as cladding layer, or on purely inorganic fluoride nanoparticles[120]. Compared to erbium-doped fiber amplifiers (EDFA), EDWAs feature higher gain and smaller size, which makes easier their integration in complex optoelectronic systems. When it comes to organic polymers, the main problem is to dissolve the erbium ion into them so that complexes with organic ligands have been often tested, with the disadvantages mentioned above about small intrinsic quantum yield[11]. Other important points are processability and the method of fabrication of the device. A solution-processable Er^{III}/Yb^{III} complex has been tested by Zhang and collaborators. In order to avoid too large concentration of Ln^{III} ions, the complex $[Er_{1.2}Yb_{0.8}(\mathbf{PBA})_6(Phen)_2]$ has been spin-coated into 10 μm-wide, 6 μm-deep grooves engraved into the SU-8 polymer (Scheme 3, Fig. 8). In this way, an optical gain of 5.2 dB was obtained at 1.55 μm with a 0.3 mW input signal and a pump power of 128 mW (976 nm) for a 15-mm long device.[119] Alternatively, the SU-8 cladding layer can be replaced with polymethyl-methacrylate (PMMA), which leads to an optical gain of 6.5 dB with an input signal of 1 mW and for a 12-mm long device.

Another approach to polymer EDWA is to dope 0.1 wt.% oleic-acid coated $NaY_{0.78}Er_{0.02}Yb_{0.20}F_4$ nanocrystals with 10-nm diameter into the photoresist epoxy polymer KMPR®. For a very small signal input of 150 nW, an optical gain of 4.8 dB/cm was obtained at 1.535 μm with a pump power of

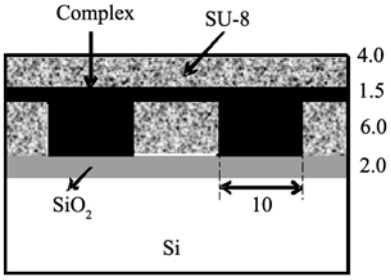

Fig. 8 Cross section of the embedded waveguide amplifier; numbers represent dimensions in μm. Redrawn from Ref. [119]

150 mW[120]. Although interesting, these new approaches to EDWAs still fail to match the highest gain reported, 7.2 dB/cm, with a polymer epoxy resin derived from SU-8[121].

A Nd^{III} waveguide laser based on rare-earth sesquioxides has also been proposed, which emits around 1.08 μm with an efficiency of 0.5% versus incident pump power[122].

4 NIR-based bio-analyses and bio-imaging

Trivalent lanthanide ions, Ln^{III}, present a viable alternative to organic luminescent stains since they enable easy spectral and time discrimination of their emission bands which span both the visible and NIR ranges. The first staining of biological cells with visible-emitting europium ions dates back to 1969 while diagnostic of malignant tumors by Yb^{III}-generated NIR light was achieved 20 years later[123]. However, further experiments had to wait until the end of the 20th century when time-gated luminescence microscopes became more routinely available[124]. In fact, attention on luminescent lanthanide bioprobes started in the mid-1970s when Finnish researchers in Turku proposed Eu^{III}, Sm^{III}, Tb^{III}, and Dy^{III} polyaminocarboxylates and β-diketonates as luminescent sensors in time-resolved luminescent (TRL) immunoassays. Although theoretically known for its specific advantages, the use of NIR light for such analyses only started to be ubiquitous with the development of upconverting nanophosphors (UCNPs, Fig. 9)[18]. Overall, lanthanide optical bioprobes are presently receiving hefty attention which is reflected in the numerous reviews which appeared in 2009–2010[3,6,7,18,125–136], including three by the authors of this article[4,5,135]. We therefore only intend to give some indications on what are the main avenues of developments for NIR lanthanide luminescent bioprobes (NIR-LLBs), not covering analytical sensors, e.g. for amino acid[137] or DNA[91] analysis.

In fact three main strategies are pursued. One simply intends to excite visible-emitting Ln^{III} ion either by upconversion[6,18] or by other multiphoton processes[4,5,126,138–142]. Another one excites NIR-emitting ion with UV or visible light[143,144] and the third one, which possesses the best future

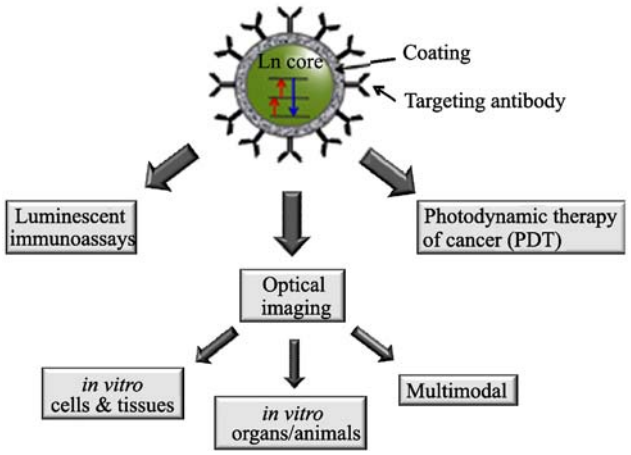

Fig. 9 Bio-analytical and bio-medical applications of lanthanide-containing upconverting nanoparticles[6]

potential, takes advantage of both NIR excitation and NIR emission[145]. Altogether, the use of nanoparticles or nanophosphors is generalizing for both bioanalysis and bioimaging applications, as well as for the photodynamic therapy of cancer (PDT). The latter was demonstrated in 2007 on MCF-7/AZ breast cancer cells; in this experiment, irradiation of $NaYF_4$:Yb,Er UCNPs by 976-nm light produces strong visible emission at 537 and 635 nm which photosensitizes a dye molecule (merocyanine 540) coated on the nanoparticles and fitted with a mouse monoclonal antibody specific to the antigen expressed by the cancerous cells; the singlet oxygen produced then destroys the cell[146]. The use of UCNPs for PDT purposes is described in the review by Wang et al[6].

As for the sector of telecommunications, there have been several attempts to improve the photophysical properties of NIR-emitting lanthanide complexes and nanoparticles with potential for bio-applications. Bioanalysis and bioimaging are often conducted either in aqueous solutions at physiological pH or, when performed *in vivo*, in presence of water. Therefore when the NIR-emitting centers are not embedded into nanoparticles, it is essential to have highly protective coordination environments. Such surroundings are for instance provided by the tetradentate and octadentate podands H_2**5a** and H_4**5b** (Scheme 4): the [Yb(**5a**)(H**5a**)] and [Yb(H_3**5b**)]Cl_2 complexes are very stable, with pYb=18.8 and 21.9, respectively, the hydration number determined by the lifetime method[32] is in the range q=0.4–0.6, and the overall quantum yield amounts to 0.22% for the bis(chelate). The corresponding Nd^{III} complexes are more hydrated (q= 0.7–1.0) so that photophysical properties are less attractive[103]. On the other hand, Nd^{III} complexes with ligands H_2**6a-d** (Scheme 4) have overall quantum yields ranging between 0.12% and 0.20% in DMSO at room temperature[147]. The tetrakis(β-diketonate) complex (**DEASPI**)[$Eu(tta)_4$] displays a one-photon quantum yield of 28% upon excitation

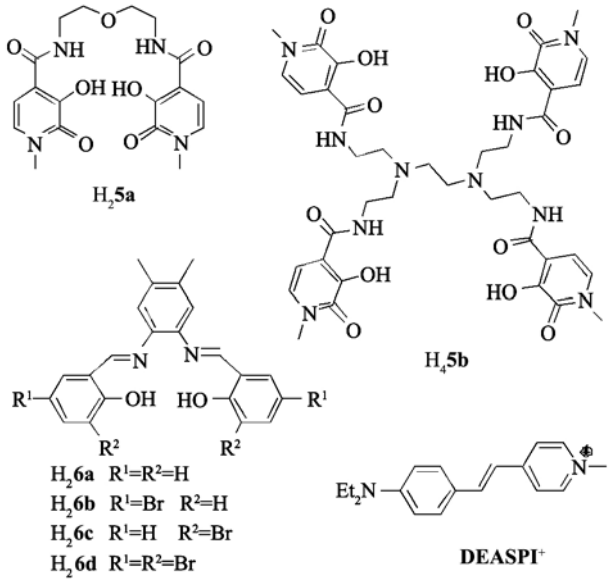

Scheme 4 Ligands for efficient NIR-emitting complexes for bio-applications

into the organic cation. Since the latter has a large two-photon absorption cross section, red emission from Eu^{III} is seen upon excitation at 1.06 μm, that is into **DEASPI**$^+$; energy transfer onto the lanthanide ions occurs via the help of a conveniently located ILCT state[144].

The bulk of recent papers devoted to improving photophysical properties of NIR-emitting lanthanide-containing bioprobes is concerned with nanoparticles (NPs)[6,26,148], especially that color-tuning is easily achieved by modifying the shape and composition of the nanoparticles, the type of emitting ion and its concentration[149–152]. The effect of inserting ions or complexes into NPs on the photophysical properties depends on many factors; it is however expected that the emitting ions will benefit from a better shielding environment and that lifetimes and quantum yields will be enhanced. This is however not always the case as exemplified by [Yb(H_3**thqtcn**-SO_3)] (Scheme 1) for which lifetime in water increases from 2 to 4 μs, but not the quantum yield[101].

Ternary complexes [Ln$(DBM)_3$(**Phen-Si**)] (Ln=Nd, Yb) have been doped into silica-coated magnetic Fe_3O_4 mesoporous nanospheres. The resulting nanocomposites display superparamagnetic properties at room temperature as well as ligand-sensitized NIR luminescence, making them candidates for dual bioprobes[153], similarly to the Gd_2O_3:Ln (Ln=Tb, Er, Yb) nanorods[154]. Another strategy for such dual probes involves crosslinker anchoring followed by ozonolysis[155]. Förster resonant energy transfer (FRET), a common methodology in bio-analyses[156], has been observed between $NaYF_4$:Yb,Er nanocrystals and quantum dots (QD): the green Er^{III} emission at 540 nm is quenched by QDs with an efficiency of about 15%, while orange emission from the latter appears. This leads to various color changes depending on the relative concentration of the QD with respect to the nanoparticles; on the other hand, Förster radius remains small (≈1.5 nm) in view of the low quantum yield of the emitting Ln^{III} ion[157]. Finally, an interesting NIR-NIR system has been proposed in which poly(acrylic acid)-functionalized YF_3:Yb,Er nanocrystals emit intense NIR light at 831 nm upon 980-nm excitation. The particles can be easily dispersed in water due to the poly(acrylic acid) coating, another asset for bio-applications[158]. It is also worth mentioning that nanoparticles based on hexagonal β-$NaYF_4$ have usually higher upconversion yield than cubic-phase nanoparticles and that surface treatment, e.g. with thioglycolic acid to make them more hydrophilic, influences the emission intensity of the blue and red emission lines relative to the green one[159].

As the needs in medical diagnostic imaging increase[160], several successful NIR bio-imaging experiments have been reported recently. In the integrated polyscale (microscopic and macroscopic) NIR bioimaging system proposed by Soga, PEG-coated Y_2O_3:Er nanoparticles excited at 980 nm conveniently image macrophage cells and the small *Caernorhabditis elegans* (*C.elegans*) worm[19]. While upconverted emission was detected in the visible in the former case, the *C.elegans* image was recorded by monitoring the 1.55 μm

emission or Er^{III}; this macroscopic imaging system is therefore of the NIR-NIR type. Subsequently the nanoparticles were encapsulated into liposomes followed by suitable derivatization of the surface with PEG, biotin or anionic or cationic agents to facilitate delivery of the luminescent stains to the targeted part (or organ) of the biological system, as demonstrated by the imaging of mouse liver[145]. The biodistribution of polyacrylic acid coated UCNPs in several mouse organs has been determined, and these NPs did not have any adverse effect on the health of the tested mice after 115 days, which suggests the feasibility of long-term targeted imaging and therapy studies[161]. The superiority of a NIR-NIR imaging system over a NIR-VIS one has been demonstrated by Kobayashi and collaborators: the lymphatic system of mice can be imaged by β-$NaYF_4$:Yb,Tm (UC-NIR) nanoparticles detected at 800 nm under various circumstances, *in vivo*, *in situ* (during surgery), and *ex vivo*; on the other hand, β-$NaYF_4$:Yb,Er (UC-green) nanoparticles detected at 550 nm are only effective in the *in situ* mode[162].

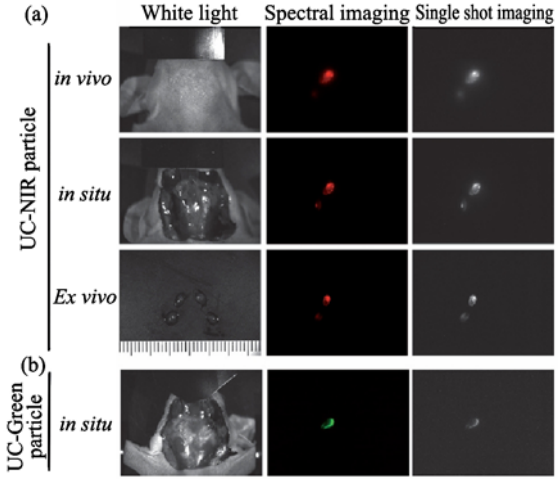

Fig. 10 Luminescence lymphatic imaging of mice with upconverting nanocrystals (see text). Reproduced with permission from Ref.[162], © The Royal Society of Chemistry 2009

UCNPs can be easily conjugated to antibodies for the targeted immunodetection of cancerous cells; for instance, $NaYbF_4$:Ln nanoparticles (Ln=Er, Ho, Tm) conjugated to the rabbit anti-CEA8 antibody specifically illuminate HeLa cells, while non-conjugated probes do not yield any signal[163].

Conjugation is however not always necessary. Simple coating of β-$NaYF_4$:Yb,Er nanophosphors with amphiphilic polymers allows good dispersion in water without loss of photophysical properties and non-specific endocytosis by cells such as NIH 3T3 murine fibroblasts, followed by their illumination[164]. Imaging properties can also be combined with therapeutic effects. Cerium oxide nanoparticles (CNP) are known to scavenge free radicals and function as antioxidants. CNPs doped with Yb^{III} and Er^{III} display upconversion behavior and can image cells; however, under *in vitro* cell culture conditions, the cellular interactions of this nanomaterials are different between normal and cancerous cells: cell proliferation is decreased for tumor cells, CNPs inducing apoptosis by producing reactive oxygenated species[165].

Rare-earth upconverting nanoparticles versus quantum dots

The advantages of lanthanide-based bioprobes over organic stains are well established and have been quantitatively delineated[166]. On the other hand, in parallel to the advent of UCNPs, NIR quantum dots (NIR QDs) have been proposed for imaging purposes and are presently a major focus of research. It is however still difficult to assess their advantages/disadvantages with respect to UCNPs from the existing literature. The various types of available NIR QDs as well as modifications of their surface are described in detail in a recent comprehensive review[167]. Assets of quantum dots are their large absorption coefficients and easy tunability of their emission by varying their size. As a result, multicolor, multiplex system can be tailored. On the other hand, blinking of the emission signal, relatively low photostability, and the toxicity of QD components (e.g. CdTe, CdSe), are real concerns which do not affect UCNPs[164]. When it comes to purely photophysical assessment, an objective comparison is now at hands for a multiplexed *in vivo* upconversion bioimaging experiment. The lymphatic drainage in the neck and the trunk of mice has been monitored by six suitably coated UCNPs emitting at different wavelengths, resulting in the lighting of six lymph nodes, each with two different colors. In a direct comparison of the efficiency of UCNPs versus QDs by determination of the detection limit of the luminescent stains, UCNPs proved to be at least **one order of magnitude** more sensitive than QDs[168]. This is of course good news for lanthanide luminescent bioprobes, which however will have to be confirmed on other systems.

5 Improving the yield of solar energy conversion

Simple in its principle, solar energy conversion encounters difficult technical problems which encompass several aspects. The first one is the spectral distribution of solar energy and its variation with the degree of cloudiness and the time of the day. For the standard AM1.5G solar spectrum, the total available power is 982 W/m^2 under clear sky, but only 166 W/m^2 under overcast sky. The relative fractions of UV, visible, and NIR light also vary with meteorological conditions (Table 3). Fig. 11 exemplifies the problem in the case of a thick silicon wafer which absorbs only about 60% of the available power. Of course, all of the absorbed light is not converted into electrical power. Lattice thermalization, recombination, junction, and contact voltage losses reduce the overall efficiency of silicon-based solar cells to a theoreti-

Table 3 Spectral irradiances and fractions thereof available for silicon absorption, downconversion (DC), and upconversion (UC), in W/m^2[169]

Weather	Total intensity	*I*(<1.15 μm)	Absorbed by Si	*I*(<0.55 μm), DC	*I* (1.15–2.21 μm), UC
Clear	982	807	468	149 (32%)	164 (35%)
Overcast	166	149	86	31 (36%)	18 (21%)

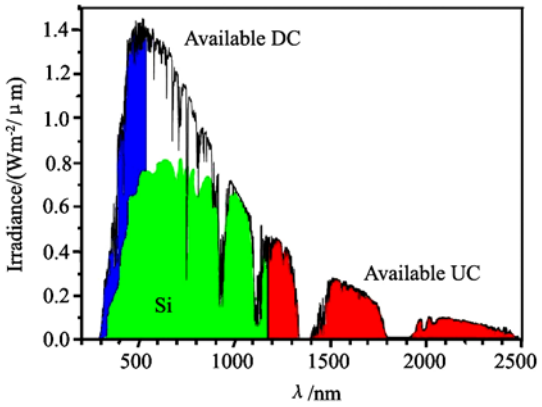

Fig. 11 AM1.5G solar spectrum together with fractions absorbed by thick silicon cells and available for down- (DC) and up- (UC) conversion. Redrawn from Ref. [169]

cally calculated limit of 31% (Shockley-Queisser limit)[169]. Presently, the best practical performance is around 25% for single crystalline Si, 11–17% for Si thin films, and ≈10% for amorphous Si[170].

In 1979, Dexter proposed to add an organic dye to semi-conductor solar cells which would harvest UV light, transfer the absorbed energy, and therefore improve the efficiency of the devices[171]. The use of rare earths in photovoltaics was pioneered by Munz et al.[172] and Reisfeld[173,174] shortly after this idea was formulated. The first attempts to increase the yield of energy conversion dealt with so-called downconversion (DC) in which a UV photon is transformed into a visible one, and involved both organic[175] and inorganic[176] compounds. For instance, surface coating of Si cells with organically modified silicate (ORMOSIL) containing $[Eu(phen)_2]Cl_3$ or $[Tb(bpy)_2]Cl_3$ results in a relative increase in the energy conversion of about 18% for crystalline Si and 8% for amorphous Si. A smaller increase was reported for a Si cell coated with a 1 mm-thick film of PVA doped with 10% $[Eu(phen)_2](NO_3)_3$, about 1% in absolute value[177]. Some Ln^{III} ions also undergo the process of quantum cutting (QC) in which one energetic UV photon is "cut" or down-converted into two visible or NIR ones[29,178]. Quantum yields between 160% and 190% are now routinely achieved while they are sometimes close to 200%[12], for instance for $LiGdF_4$ doped with Eu^{III}[29]. How much can be gained by this type of process? Trupke and collaborators have theoretically assessed the gain which could be obtained by DC for non- concentrated solar illumination (6000 K) and in function of the solar cell's band gap energy (E_g). For E_g= 1.1 eV, the Shockley-Queisser limit of 31% is extended to ≈37% when the converter is located at the front surface of the solar cell, but if the converter is built onto the rear surface, this limit goes up to ≈40%[179].

Quantum cutting with rare-earth doped materials proceeds according to three different mechanisms[180]. (i) Generation of electron-hole (e-h) pairs in the lattice, but production of a second pair in Si requires an electron energy of at least 2.6 eV, so that the increase in the internal quantum efficiency is small (<5% for λ=350 nm), unless short wavelength are used (50% at λ=250 nm). (ii) Generation of two visible photons in a single rare earth ion, such as Pr^{III}; when the $^1S_0$ level is excited, at 185 nm, this ion emits a blue (405 nm) and a red photon (620 nm) with an efficiency of 140%. (iii) Down-conversion with rare-earth pairs; for instance, absorption of one UV photon by Gd^{III} followed by partial transfer of the energy onto Eu^{III} by cross relaxation and by regular energy transfer of the remaining part so that two 612-nm photons are emitted with an internal quantum efficiency close to 200%. However, due to very weak absorption of Gd^{III}, the overall (or external) quantum efficiency is only around 32%; this can be substantially improved, up to 110%, by co-doping Er^{III} and using Tb^{III} instead of Eu^{III}. The spectroscopy of a wealth of QC lanthanide-containing systems is presently being thoroughly investigated in view of their potential applications in Si solar cells[181–184].

Returning to Fig. 11 and Table 3, one realizes that not only the UV portion of the solar spectrum is available for DC and QC, but a good deal of the NIR emission could be transformed into visible light by UC[15,169,185]. In this process, two photons with energy $\frac{1}{2}E_g \le h\nu < E_g$ (E_g is the bandgap of the semi-conductor) create one photon with $h\nu \ge E_g$, a process available for many lanthanide ions[25]. In fact, combining the available powers for both DC (+QC) and UC amounts to about half of the total available sun irradiance. Therefore it is obvious that both methods of improving the yield of solar cells should be implemented simultaneously. The transitions available for DC (QC) and UC in rare-earth ions are listed in Table 1 and numerous up-converting materials, usually involving Er^{III}, have been proposed for Si solar cells[186]. As far as conversion yield improvement is concerned, a detailed analysis is available, which takes into account both UC and, instead of DC, a more efficient process called multi-exciton generation (MEG) from quantum dots with composition PbS, PbSe, PbTe or CdSe, in which one photon with energy $h\nu \ge E_g$ yields n e-h pairs with energy $\ge E_g$. With optimistically assumed maximum yields for MEG (70%) and UC (25%), the theoretical photovoltaic conversion efficiency for a single bandgap solar cell reaches ≈40%. The main problem with UC is that it is non-linear process, usually initiated by intense laser irradiation, while solar light is diffuse[187]. Efforts are therefore given attention to build solar concentrator layers to overcome this difficulty. In turn, MEG is constrained by competing de-excitation processes, recombination of excitons without charge separation, and high-impact ionization threshold, so that much work remains to be done before the ≈40% limit can be practically achieved[188].

Dye-sensitized solar cells

Another approach to solar energy conversion has been pioneered by Grätzel who proposed the sensitization of mesoscopic oxide films with wide band gaps by organic dyes or quantum dots[189]. Anatase (TiO_2) is commonly used under the form of nanoparticles and a monolayer of the sen-

sitizer is deposited on their surface. Photoexcitation injects electrons into the conduction band of the oxide and the dye is regenerated by electron donation from an electrolyte, an organic solvent containing the iodide/tri-iodide redox couple. A main advantage of these devices is their easy processability allied to transparency so that films can be produced for various coatings, e.g. window coating. Up to now, laboratory-size (1 cm^2) dye-sensitized solar cells (DSSCs) have reached an overall solar-to-electrical conversion efficiency slightly over 11% while practical modules (25–100 cm^2) reach 8%[170].

This type of cell suffers from the same drawback as Si cells in that UV and NIR light are difficult to harvest and many attempts have been made to improve the situation since DSSCs feature several parameters which can be optimized, such as the dye sensitizer, metal oxide band gap, nature of the electrolyte and redox couple, wavelength converter additives, for instance. Although still in its infancy, the use of lanthanide-containing materials in DSSCs starts gaining momentum. For instance, bulk hetero-junction cells fabricated from free base phthalocyanine and samarium phthalocyaninato double and triple deckers as electron donors and a perylenediamine derivative as electron acceptor have the capability of broad-band light harvest, from NIR to UV, but the overall efficiency remains small and such cells will need extensive optimization before they can really be considered as practical light-converting devices[190]. Another approach has been pioneered by Kim et al., who has introduced a europium complex as energy-converting material in a DSSC working with the reference dye N719 and who reported an improvement of about 10% in the conversion efficiency due to DC[191]. There is no doubt that these avenues will be pursued, together with the introduction of UC materials and will therefore help bringing DSSCs closer to wide use in day-to-day life, although a cost/effectiveness analysis will have to be carried out in view of the price and rarefaction of rare-earth resources[192] and of the effectiveness of d-transition metal ion complexes as solar concentrator materials[193].

6 Perspectives

The applications discussed above demonstrate the power of lanthanide NIR luminescence in a wide range of fields, from telecommunications to medicine and solar energy. While silica-based telecommunication devices are well established and understood, many efforts are still needed to come up with effective polymer-based waveguide amplifiers. The use of NIR-emitting lanthanide ions is more recent in biosciences, particularly for *in vivo* imaging experiments; presently, scientists devote a lot of attention to the tailoring of dual-probe UCNPs for simultaneous MRI and optical imaging[194,195]. Much more remains to be done in the field of solar cells for which converting materials not only must meet stringent photophysical properties but also present adequate processability and cost/effectiveness ratio. Altogether, there is however no doubt that the versatile spectroscopic properties of lanthanides will have to be seriously considered as alternatives to other technologies (or in complement to them) in these various fast developing areas, so that we anticipate a hefty growth in NIR lanthanide research in a very near future.

Acknowledgment: This research is supported through grants from the Swiss National Science Foundation; JCB thanks the WCU program from the National Science Foundation of Korea for grant R31-10035; SE thanks FWO-Flanders for a Postdoctoral Fellowship.

References:

[1] Bünzli J C G, Comby S, Chauvin A S, Vandevyver C D B. New opportunities for lanthanide luminescence. *J. Rare Earths*, 2007, **25**: 257.

[2] Suzuki H. Organic light-emitting materials and devices for optical communication technology. *J. Photochem. Photobiol., A,* 2004, **166**: 155.

[3] Chen Z Q, Bian Z Q, Huang C H. Functional Ir-III complexes and their applications. *Adv. Mater.,* 2010, **22**: 1534.

[4] Eliseeva S V, Bünzli J C G. Lanthanide luminescence for functional materials and bio-sciences. *Chem. Soc. Rev.,* 2010, **39:** 189.

[5] Bünzli J C G. Lanthanide luminescence for biomedical analyses and imaging. *Chem. Rev.,* 2010, **110**: 2729.

[6] Wang F, Banerjee D, Liu Y S, Chen X Y, Liu X G. Upconversion nanoparticles in biological labeling, imaging, and therapy. *Analyst*, 2010, **135:** 1839.

[7] Uh H, Petoud S. Novel antennae for the sensitization of near infrared luminescent lanthanide cations. *Comptes Rendus Chimie,* 2010, **13**: 668.

[8] Bünzli J C G, Chauvin A S, Vandevyver C D B, Song B, Comby S. Lanthanide bimetallic helicates for *in vitro* imaging and sensing. *Ann. N. Y. Acad. Sci.,* 2008, **1130**: 97.

[9] Amiot C L, Xu S P, Liang S, Pan L Y, Zhao J X J. Near-infrared fluorescent materials for sensing of biological targets. *Sensors*, 2008, **8**: 3082.

[10] Cooper D E, D'Andrea A, Faris G W, MacQueen B, Wright W H. Up-converting phosphors for detection and identification using antibodies. Van Emon J M, Ed. Immunoassay and Other Bioanalytical Techniques. Boca Raton: CRC Press, Taylor & Francis group, 2007, Ch. 9, 217-47.

[11] Comby S, Bünzli J C G. Lanthanide near-infrared luminescence in molecular probes and devices, Gschneidner K A Jr, Bünzli J -C G, Pecharsky V K, Eds. Handbook on the Physics and Chemistry of Rare Earths. Amsterdam: Elsevier Science B.V., 2007, 37, Ch. 235.

[12] Zhang Q Y, Huang X Y. Recent progress in quantum cutting phosphors. *Prog. Mater. Sci.,* 2010, **55**: 353.

[13] van der Ende B M, Aarts L, Meijerink A. Lanthanide ions as spectral converters for solar cells. *Phys. Chem. Chem. Phys.,* 2009, **11**: 11081.

[14] Andrews D L. Energy harvesting: a review of the interplay between structure and mechanism. *J. Nanophoton.,* 2008, **2**: Art. Nr. 022502.

[15] Strümpel C, McCann M, Beaucarne G, Arkhipov V, Slaoui A,

Svrcek V, del Canizo C, Tobias I. Modifying the solar spectrum to enhance silicon solar cell efficiency--An overview of available materials. *Solar En. Mat. Sol. Cells*, 2007, **91**: 238.

[16] Shalav A, Richards B S, Green M A. Luminescent layers for enhanced silicon solar cell performance: Up-conversion. *Solar En. Mat. Sol. Cells,* 2007, **91**: 829.

[17] Shen J, Sun L D, Yan C H. Luminescent rare earth nanomaterials for bioprobe applications. *Dalton Trans.,* 2008, (42): 5687.

[18] Li C X, Lin J. Rare earth fluoride nano-/microcrystals: synthesis, surface modification and application. *J. Mater. Chem.,* 2010, **20**: 6831.

[19] Soga K. Development of NIR fluorescence bioimaging system through polyscale technology. *Bunseki Kagaku,* 2009, **58**: 461.

[20] Minowa T. Rare earth magnets: conservation of energy and the environment. *Res. Geol.,* 2008, **58**: 414.

[21] Miller G J. Complex rare-earth tetrelides, $RE_5(Si_xGe_{1-x})_4$: New materials for magnetic refrigeration and a superb playground for solid state chemistry. *Chem. Soc. Rev.,* 2006, **35**: 799.

[22] Gschneidner Jr. K A, Pecharsky V K, Pecharsky A O. Recent development in magnetocaloric materials. *Rep. Prog. Phys.,* 2005, **68**: 1479.

[23] Iqbal M J, Ahmad Z. Electrical and dielectric properties of lithium manganate nanomaterials doped with rare-earth elements. *J. Power Sources,* 2008, **179**: 763.

[24] Xu J Y, Zhang Y, Yan R X, Luo Y C. New research progress in investigation of AB5 rare earth-based hydrogen storage alloys in Ni-MH battery. *Chinese Journal of Power Source* (in Chin.)*,* 2009, **33**: 923.

[25] Auzel F. Upconversion and Anti-Stokes processes with f and d ions in solids. *Chem. Rev.,* 2004, **104**: 139.

[26] Wang F, Liu X. Recent advances in the chemistry of lanthanide-doped upconversion nanocrystals. *Chem. Soc. Rev.,* 2009, **38**: 976.

[27] Petoud S. Annual meeting, COST Action D38, Warsaw, April 25-27, 2009, abstract O1 2009.

[28] Comby S, Imbert D, Vandevyver C D B, Bünzli J C G. A novel strategy for the design of 8-hydroxyquinolinate-based lanthanide bioprobes emitting in the NIR range. *Chem. Eur. J.,* 2007, **13**: 936.

[29] Wegh R T, Donker H, Oskam K D, Meijerink A. Visible quantum cutting in $LiGdF_4$: Eu^{3+} through down conversion. *Science,* 1999, **283**: 663.

[30] Carnall W T. The absorption and fluorescence spectra of rare earth ions in solution. Gschneidner K A Jr, Eyring L, Eds. Handbook on the Physics and Chemistry of Rare Earths. Amsterdam: North Holland Publ. Co., 1979, Vol. 3, Ch.24.

[31] Soga K, Wang W Z, Riman R E, Brown J B, Mikeska K R. Luminescent properties of nanostructured Dy^{3+}- and Tm^{3+}-doped lanthanum chloride prepared by reactive atmosphere processing of sol-gel derived lanthanum hydroxide. *J. Appl. Phys.,* 2003, **93**: 2946.

[32] Bünzli J C G, Eliseeva S V. Basics of lanthanide photophysics. Lanthanide luminescence: Photophysical, analytical and biological aspects. Hänninen P, Härmä H, Eds. Spinger Series on Fluorescence. Berlin: Springer Verlag, 2010, Vol. 8, Ch. published on line July 15. DOI 10.1007/4243_2010_3.

[33] Bünzli J C G, Chauvin A S, Kim H K, Deiters E, Eliseeva S V. Lanthanide luminescence efficiency in eight- and nine-coordinate complexes: role of the radiative lifetime. *Coord. Chem. Rev.,* 2010, **254**: 2623.

[34] Walsh B M. Judd Ofelt theory: principles and practices. Bartolo B Di, Forte O, Eds. Advances in Spectroscopy for Lasers and Sensing. Berlin: Springer Verlag, 2006, 403-33.

[35] Görller-Walrand C, Binnemans K. Spectral intensities of f-f transitions. Gschneidner K A Jr, Eyring L, Eds. Handbook on the Physics and Chemistry of Rare Earths. Amsterdam: Elsevier Science B. V., 1998, Vol. 25, Ch.167.

[36] Görller-Walrand C, Fluyt L, Ceulemans A, Carnall W T. Magnetic dipole transitions as standards for Judd-Ofelt parametrization in lanthanide spectra. *J. Chem. Phys.,* 1991, **95**: 3099.

[37] Lazarides T, Sykes D, Faulkner S, Barbieri A, Ward M D. On the mechanism of d-f energy transfer in Ru(II)/Ln(III) and Os(II)/Ln(III) dyads: Dexter-type energy transfer over a distance of 20 angstrom. *Chem. Eur. J.,* 2008, **14**: 9389.

[38] Wong W K, Zhu X, Wong W Y. Synthesis, structure, reactivity and photoluminescence of lanthanide(III) monoporphyrinate complexes. *Coord. Chem. Rev.,* 2007, **251**: 2386.

[39] Korovin Y V, Rusakova N V. Infrared 4f-luminescence of lanthanides in the complexes with macrocyclic ligands. *Rev. Inorg. Chem.,* 2001, **21**: 299.

[40] Dos Santos C M G, Harte A J, Quinn S J, Gunnlaugsson T. Recent developments in the field of supramolecular lanthanide luminescent sensors and self-assemblies. *Coord. Chem. Rev.,* 2008, **252**: 2512.

[41] Rusakova N, Semenishyn N, Korovin Y. Heteronuclear lanthanide-containing complexes on the base of modified porphyrins and their luminescent properties. *J. Porph. Phthalocyan.,* 2010, **14**: 166.

[42] Wang Q M, Sasaki S, Tamiaki H. Near-infrared luminescence from ytterbium(III) ternary complexes by visible-light excitation of attached chlorophyll derivatives. *Chem. Lett.,* 2009, **38**: 648.

[43] Placidi M P, Natrajan L S, Sykes D, Kenwright A M, Faulkner S. Bimetallic lanthanide complexes derived from macrocycle-appended m-xylyl derivatives: synthesis and spectroscopic properties. *Helv. Chim. Acta,* 2009, **92**: 2427.

[44] Andrews M, Ward B D, Laye R H, Kariuki B M, Pope S J A. Sensitized lanthanide-ion luminescence with aryl-substituted N-(2-Nitrophenyl)acetamide-derived chromophores. *Helv. Chim. Acta,* 2009, **92**: 2159.

[45] Crosby G A, Kasha M. Intramolecular energy transfer in ytterbium organic chelates. *Spectrochim. Acta*, 1958, **10**: 377.

[46] Tsvirko M P, Meshkova S B, Venchikov V Y, Topilova Z M, Bol'shoi D V. Determination of contributions of various molecular groups to nonradiative deactivation of electronic excitation energy in β-diketonate complexes of ytterbium(III). *Opt. Spectrosc. (Engl. Transl.),* 2001, **90**: 669.

[47] Wei F, Li Y Z, Ran G Z, Qin G G. 1.54 μm electroluminescence from p-Si anode organic light emitting diode with Bphen: $Er(DBM)_3$phen as emitter and Bphen as electron transport material. *Optics Express*, 2010, **18**: 13542.

[48] Dang S, Yu J B, Wang X F, Guo Z Y, Sun L N, Deng R P, Feng J, Fan W Q, Zhang H J. A study on the NIR-luminescence emitted from ternary lanthanide [Er(III), Nd(III) and Yb(III)] complexes containing fluorinated-ligand and 4,5-diazafluoren-9-one. *J. Photochem. Photobiol. A Chem.,* 2010, **214**: 152.

[49] Gillin W P, Curry R J. Erbium (III) tris(8-hydroxyquinoline) (ErQ): A potential material for silicon compatible 1.5 μm emit-

ters. *Appl. Phys. Lett.,* 1999, **74**: 798.
[50] Khreis O M, Curry R J, Somerton M, Gillin W P. Infrared organic light emitting diodes using neodymium tris-(8-hydroxyquinoline). *J. Appl. Phys.,* 2000, **88**: 777.
[51] Khreis O M, Gillin W P, Somerton M, Curry R J. 980 nm electroluminescence from ytterbium tris(8-hydroxyquinoline). *Org. Electr.,* 2001, **2**: 45.
[52] Albrecht M, Osetska O, Klankermayer J, Fröhlich R, Gumy F, Bünzli J C G. Enhancement of near-IR emission by bromine substitution in lanthanide complexes with 2-carboxamide-8-hydroxyquinoline. *Chem. Commun.,* 2007, (18): 1834.
[53] Shavaleev N M, Scopelliti R, Gumy F, Bünzli J C G. Surprisingly bright near-infrared luminescence and short radiative lifetimes of ytterbium in hetero-binuclear Yb-Na chelates. *Inorg. Chem.,* 2009, **48**: 7937.
[54] Samuel J, Tallec G, Cherns P, Ling W L, Raccurt O, Poncelet O, Imbert D, Mazzanti M. Lanthanide-chelate silica nanospheres as robust multicolor Vis-NIR tags. *Chem. Commun.,* 2010, **46**: 2647.
[55] Nonat A, Imbert D, Pécaut J, Giraud M, Mazzanti M. Structural and photophysical studies of highly stable lanthanide complexes of tripodal 8-hydroxyquinolinate ligands based on 1,4,7-triazacyclononane. *Inorg. Chem.,* 2009, **48**: 4207.
[56] He H, May P S, Galipeau D. Monoporphyrinate ytterbium(III) complexes with new ancillary ligands: synthesis, structural analysis and photophysical investigation. *Dalton Trans.,* 2009, (24): 4766.
[57] Albrecht M, Osetska O, Bünzli J C G, Gumy F, Fröhlich R. Homo- and heterodinuclear helicates of lanthanide(III), zinc(II) and aluminium(III) based on 8-hydroxyquinoline ligands. *Chem. Eur. J.,* 2009, **15**: 8791.
[58] Hebbink G A, Grave L, Woldering L A, Reinhoudt D N, Van Veggel F C J M. Unexpected sensitization efficiency of the near-infrared Nd^{3+}, Er^{3+}, and Yb^{3+} emission by fluorescein compared to eosin and erythrosin. *J. Phys. Chem. A,* 2003, **107**: 2483.
[59] Zhang J, Badger P D, Greib S J, Petoud S. Sensitization of near-infrared-emitting lanthanide cations in solution by tropolonate ligands. *Angew. Chem. Int. Ed.,* 2005, **44**: 2508.
[60] Zhang J, Petoud S. Azulene-moiety-based ligand for the efficient sensitization of four near-infrared luminescent lanthanide cations: Nd^{3+}, Er^{3+}, Tm^{3+}, and Yb^{3+}. *Chem. Eur. J.,* 2008, **14**: 1264.
[61] Deiters E, Gumy F, Bünzli J C G. Acridone-benzimidazole fused ligands: a new class of sensitizers of lanthanide luminescence via low-energy excitation. *Eur. J. Inorg. Chem.,* 2010, **2010**: 2723.
[62] Carlos L D, Ferreira R A S, Bermudez V D, Ribeiro S J L. Lanthanide-containing light-emitting organic-inorganic hybrids: A bet on the future. *Adv. Mater.,* 2009, **21**: 509.
[63] Guillou O, Daiguebonne C. Lanthanide-containing coordination polymers. Gschneidner K A Jr, Bünzli J C G, Pecharsky V K, Eds. Handbook on the Physics and Chemistry of Rare Earths. Amsterdam: Elsevier Science B.V., 2004, Vol. Ch. 221, Vol. 34.
[64] Haquin V, Gumy F, Daiguebonne C, Bünzli J C G, Guillou O. Structural and NIR luminescent properties of erbium-containing coordination polymers. *Eur. J. Inorg. Chem.,* 2009, (29-30): 4491.
[65] White K A, Chengelis D A, Gogick K A, Stehman J, Rosi N L, Petoud S. Near-infrared luminescent lanthanide MOF barcodes. *J. Am. Chem. Soc.,* 2009, **131**: 18069.
[66] White K A, Chengelis D A, Zeller M, Geib S J, Szakos J, Petoud S, Rosi N L. Near-infrared emitting ytterbium metal-organic frameworks with tunable excitation properties. *Chem. Commun.,* 2009, (30): 4506.
[67] Chi Y X, Niu S Y, Jin J. Syntheses, structures and photophysical properties of a series of Zn-Ln coordination polymers (Ln=Nd, Pr, Sm, Eu, Tb, Dy). *Inorg. Chim. Acta,* 2009, **362**: 3821.
[68] Hu M X, Chen Y G, Zhang C J, Kong Q J. High-dimensional frameworks dependent on coordination mode of ligand controlled by acidity of reaction solution. Syntheses, structures, magnetic and fluorescence properties of eight new compounds. *CrystEngComm,* 2010, **12**: 1454.
[69] Huang W, Wu D Y, Zhou P, Yan W B, Guo D, Duan C Y, Meng Q J. Luminescent and magnetic properties of lanthanide-thiophene-2,5-dicarboxylate hybrid materials. *Cryst. Growth Des.,* 2009, **9**: 1361.
[70] Wang H Y, Cheng J Y, Ma J P, Dong Y B, Huang R Q. Synthesis and characterization of new coordination polymers with tunable luminescent properties generated from bent 1,2,4-triazole-bridged N,N'-dioxides and Ln(III) salts. *Inorg. Chem.,* 2010, **49**: 2416.
[71] Marchal C, Filinchuk Y, Chen X Y, Imbert D, Mazzanti M. Lanthanide-based coordination polymers assembled by a flexible multidentate linker: Design, structure, photophysical properties, and dynamic solid-state behavior. *Chem. Eur. J.,* 2009, **15**: 5273.
[72] Ming Z Q, Miao Y X, Si S F. $\{Na_2[Nd_4(OX)(BDC)_6(H_2O)_6]\}_n$: A 3-D coordination polymer with hybrid dicarboxylates. *J. Coord. Chem.,* 2009, **62**: 833.
[73] Vögtle F, Gorka M, Vicinelli V, Ceroni P, Maestri M, Balzani V. A dendritic antenna for near-infrared emission of Nd^{3+} ions. *Chem. Phys. Chem.,* 2001, **2**: 769.
[74] Vicinelli V, Ceroni P, Maestri M, Balzani V, Gorka M, Vögtle F. Luminescent lanthanide ions hosted in a fluorescent polylysin dendrimer. Antenna-like sensitization of visible and near-infrared emission. *J. Am. Chem. Soc.,* 2002, **124**: 6461.
[75] Pitois C, Vestberg R, Rodlert M, Malmstrom E, Hult A, Lindgren M. Fluorinated dendritic polymers and dendrimers for waveguide applications. *Opt. Mater.,* 2003, **21**: 499.
[76] Pitois C, Hult A, Lindgren M. Lanthanide-cored fluorinated dendrimer complexes: synthesis and luminescence characterization. *J. Lumin.,* 2005, **111**: 265.
[77] Saudan C, Ceroni P, Vicinelli V, Maestri M, Balzani V, Gorka M, Lee S K, van Heyst J, Vögtle F. Cyclam-based dendrimers as ligands for lanthanide ions. *Dalton Trans.,* 2004, (10): 1597.
[78] Giansante C, Ceroni P, Balzani V, Vögtle F. Self-assembly of a light-harvesting antenna formed by a dendrimer, a Ru(II) complex, and a Nd(III) ion. *Angew. Chem. Int. Ed.,* 2008, **47**: 5422.
[79] Oh J B, Nah M K, Kim Y H, Kang M S, Ka J W, Kim H K. Er(III)-cored complexes based on dendritic Pt(II)-porphyrin ligands: Synthesis, near-IR emission enhancement, and photophysical studies. *Adv. Func. Mater.,* 2007, **17**: 413.
[80] Kim Y H, Baek N S, Oh J B, Nah M K, Roh S G, Song B J, Kim H K. Molecular design and photophysical criteria for lanthanide emission enhancement in erbium(III)-cored complexes based on dendritic ligands for information technology. *Mac-*

romol. Res., 2007, **15**: 272.

[81] Oh J B, Kim Y H, Nah M K, Kim H K. Inert and stable erbium(III)-cored complexes based on metalloporphyrins bearing aryl-ether dendron for optical amplification: synthesis and emission enhancement. *J. Lumin.,* 2005, **111**: 255.

[82] Ward M D. Transition-metal sensitised near-infrared luminescence from lanthanides in d-f heteronuclear arrays. *Coord. Chem. Rev.,* 2007, **251**: 1663.

[83] Bünzli J C G, Piguet C. Taking advantage of luminescent lanthanide ions. *Chem. Soc. Rev.,* 2005, **34**: 1048.

[84] Faulkner S, Natrajan L S, Perry W S, Sykes D. Sensitised luminescence in lanthanide containing arrays and d–f hybrids. *Dalton Trans.,* 2009, (20): 3890.

[85] Piguet C, Bünzli J C G. Self-assembled lanthanide helicates: from basic thermodynamics to applications. Gschneidner K A Jr, Bünzli J C G, Pecharsky V K, Eds. Handbook on the Physics and Chemistry of Rare Earths. Amsterdam: Elsevier Science, B.V., 2010, Vol. 40, Ch. 247.

[86] Chen F F, Chen Z Q, Bian Z Q, Huang C H. Sensitized luminescence from lanthanides in d-f bimetallic complexes. *Coord. Chem. Rev.*, 2010, **254**: 991.

[87] Ward M D. Mechanisms of sensitization of lanthanide(III)-based luminescence in transition metal/lanthanide and anthracene/lanthanide dyads. *Coord. Chem. Rev.,* 2010, **254**: 2634.

[88] Tart N M, Sykes D, Sazanovich I, Tidmarsh I S, Ward M D. Iridium(III) luminophores as energy donors for sensitised emission from lanthanides in the visible and near-infrared region. *Photochem. Photobiol. Sci.,* 2010, **9**: 886.

[89] Lazarides T, Tart N M, Sykes D, Faulkner S, Barbieri A, Ward M D. $[Ru(bipy)_3]^{2+}$ and $[Os(bipy)_3]^{2+}$ chromophores as sensitisers for near-infrared luminescence from Yb(III) and Nd(III) in d/f dyads: contributions from Forster, Dexter, and redox-based energy-transfer mechanisms. *Dalton Trans.,* 2009, (20): 3971.

[90] Vazquez Lopez M, Eliseeva S V, Blanco J M, Rama G, Bermejo M R, Vazquez M E, Bünzli J C G. Sensitized visible and NIR lanthanide luminescence from Ln^{III}-DOTA-Bipy complexes and Ln^{III}-DOTA-Bipy-Ru^{II} coordination conjugates. *Eur. J. Inorg. Chem.,* 2010, **2010**: 4532.

[91] Nonat A M, Allain C, Faulkner S, Gunnlaugsson T. Mixed d-f(3) coordination complexes possessing improved near- infrared (NIR) lanthanide luminescent properties in aqueous solution. *Inorg. Chem.,* 2010, **49**: 8449.

[92] Bo Q B, Sun G X, Geng D L. Novel three-dimensional pillared-layer Ln(III)-Cu(I) coordination polymers featuring spindle-shaped heterometallic building units. *Inorg. Chem.,* 2010, **49**: 561.

[93] Zhao B, Zhao X Q, Chen Z, Shi W, Cheng P, Yan S P, Liao D Z. Structures and near-infrared luminescence of unique 4d-4f heterometal-organic frameworks (HMOF). *CrystEngComm,* 2008, **10**: 1144.

[94] Li X L, Zhang K J, Li J J, Cheng X X, Chen Z N. Dual luminescent dinuclear gold(I) complexes of terpyridyl-functionalized Alkyne ligands and their efficient sensitization of Eu^{III} and Yb^{III} luminescence. *Eur. J. Inorg. Chem.,* 2010, **2010**: 3449.

[95] Xu H B, Wen H M, Chen Z H, Li J, Shi L X, Chen Z N. Square structures and photophysical properties of Zn_2Ln_2 complexes (Ln=Nd, Eu, Sm, Er, Yb). *Dalton Trans.,* 2010, **39**: 948.

[96] Wei T, Zhao S, Bi W, Lü X, Hui Y, Song J, Wong W K, Jones R A. Co-existence of heterometallic Zn2Er and ZnEr arrayed chromophores for the sensitization of near-infrared (NIR) luminescence. *Inorg. Chem. Commun.,* 2009, **12**: 1216.

[97] Kumar G A, Riman R E, Torres L A D, Banerjee S, Romanelli A D, Emge T J, Brennan J G. Near-infrared optical characteristics of chalcogenide-bound Nd^{3+} molecules and clusters. *Chem. Mater.,* 2007, **19**: 2937.

[98] Shavaleev N M, Scopelliti R, Gumy F, Bünzli J C G. Modulating the near-infrared luminescence of neodymium and ytterbium complexes with tridentate ligands based on benzothiazole-substituted 8-hydroxyquinolines. *Inorg. Chem.,* 2009, **48**: 2908.

[99] Kumar G A, Riman R E, Torres L A D, Garcia O B, Banerjee S, Kornienko A, Brennan J G. Chalcogenide-bound erbium complexes: Paradigm molecules for infrared fluorescence emission. *Chem. Mater.,* 2005, **17**: 5130.

[100] Song L M, Hu J, Wang J S, Liu X H, Zhen Z. Novel perfluorodiphenylphosphinic acid lanthanide (Er or Er-Yb) complex with high NIR photoluminescence quantum yield. *Photochem. Photobiol. Sci.,* 2008, **7**: 689.

[101] Glover P B, Bassett A P, Nockemann P, Kariuki B M, Van Deun R, Pikramenou Z. Fully fluorinated imidodiphosphinate shells for visible- and NIR-emitting lanthanides: Hitherto unexpected effects of sensitizer fluorination on lanthanide emission properties. *Chem. Eur. J.,* 2007, **13**: 6308.

[102] Sun L N, Yu J B, Zheng G L, Zhang H J, Meng Q G, Peng C Y, Fu L S, Liu F Y, Yu Y N. Syntheses, structures and near-IR luminescent studies on ternary lanthanide (Er^{III}, Ho^{III}, Yb^{III}, Nd^{III}) complexes containing 4,4,5,5,6,6,6- heptafluoro-1-(2-thienyl)hexane-1,3-dionate. *Eur. J. Inorg. Chem.,* 2006, (19): 3962.

[103] Moore E G, Xu J, Dodani S C, Jocher C J, D'Aléo A, Seitz M, Raymond K N. 1-Methyl-3-hydroxy-pyridin-2-one complexes of near infra-red emitting lanthanides: Efficient sensitization of Yb(III) and Nd(III) in aqueous solution. *Inorg. Chem.,* 2010, **49**: 4156.

[104] Bischof C, Wahsner J, Scholten J, Trosien S, Seitz M. Quantification of C–H quenching in near-IR luminescent ytterbium and neodymium cryptates. *J. Am. Chem. Soc.,* 2010, **132**: 14334.

[105] Monguzzi A, Milani A, Lodi L, Trioni M I, Tubino R, Castiglioni C. Vibrational overtones quenching of near infrared emission in Er^{3+} complexes. *New J. Chem.,* 2009, **33**: 1542.

[106] Zheng Y, Pearson J, Tan R H C, Gillin W P, Wyatt P B. Erbium bis(pentafluorophenyl) phosphinate: a new hybrid material with unusually long-lived infrared luminescence. *J. Mater. Sci. Mater. Electron.,* 2009, **20**: 430.

[107] Hernandez I, Tan R H C, Pearson J M, Wyatt P B, Gillin W P. Nonradiative de-excitation mechanisms in long-lived erbium(III) organic compounds $Er_xY_{1-x}[(p\text{-}CF_3\text{-}C_6F_4)_2PO_2]_3$. *J. Phys. Chem. B,* 2009, **113**: 7474.

[108] Quochi F, Orru R, Cordella F, Mura A, Bongiovanni G, Artizzu F, Deplano P, Mercuri M L, Pilia L, Serpe A. Near infrared light emission quenching in organolanthanide complexes. *J. Appl. Phys.,* 2006, **99**: Art. Nr. 053520.

[109] Monguzzi A, Tubino R, Meinardi F, Biroli A O, Pizzotti M, Demartin F, Quochi F, Cordella F, Loi M A. Novel Er^{3+} perfluorinated complexes for broadband sensitized near infrared emission. *Chem. Mater.,* 2009, **21**: 128.

[110] Norton K, Kumar G A, Dilks J L, Emge T J, Riman R E, Brik

M G, Brennan J G. Lanthanide compounds with fluorinated aryloxide ligands: Near-infrared emission from Nd, Tm, and Er. *Inorg. Chem.,* 2009, **48**: 3573.

[111] Kornienko A, Emge T J, Kumar G A, Riman R E, Brennan J G. Lanthanide clusters with internal Ln ions: Highly emissive molecules with solid-state cores. *J. Am. Chem. Soc.,* 2005, **127**: 3501.

[112] Lian S, Qi Y, Rong C, Yu L, Zhu A, Yin D, Liu S. Effectively leveraging solar energy through persistent dual red phosphorescence: Preparation, characterization, and density functional theory study of $Ca_2Zn_4Ti_{16}O_{38}:Pr^{3+}$. *J. Phys. Chem. C,* 2010, **114**: 7196.

[113] Lezhnina M, Kynast U. Luminescence from tungstate functionalized sodalites involving NIR states. *J. Alloys Compd.,* 2004, **380**: 55.

[114] Zhang J, Shade C M, Chengelis D A, Petoud S. A strategy to protect and sensitize near-infrared luminescent Nd^{3+} and Yb^{3+}: organic tropolonate ligands for the sensitization of Ln^{3+}-doped $NaYF_4$ nanocrystals. *J. Am. Chem. Soc.,* 2007, **129**: 14834.

[115] dos Santos E R, Freire R O, da Costa N B, Paz F A A, de Simone C A, Junior S A, Araujo A A S, Nunes L A, de Mesquita M E, Rodrigues M O. Theoretical and experimental spectroscopic approach of fluorinated Ln^{3+}-diketonate complexes. *J. Phys. Chem. A,* 2010, **114**: 7928.

[116] Wu J, Wieligor M, Zerda T W, Coffer J L. The impact of erbium incorporation on the structure and photophysics of silicon-germanium nanowires. *Nanoscale,* 2010, Published on the web, September 2010, DOI 10.1039/C0NR00476F.

[117] Mech A, Monguzzi A, Meinardi F, Mezyk J, Macchi G, Tubino R. Sensitized NIR erbium(III) emission in confined geometries: A new strategy for light emitters in telecom applications. *J. Am. Chem. Soc.,* 2010, **132**: 4574.

[118] Chen C, Zhang D, Li T, Zhang D M, Song L M, Zhen Z. Demonstration of optical gain at 1550 nm in erbium-ytterbium co-doped polymer waveguide amplifier. *J. Nanosci. Technol.,* 2010, **10**: 1947.

[119] Chen C, Zhang D, Li T, Zhang D M, Song L M, Zhen Z. Erbium-ytterbium codoped waveguide amplifier fabricated with solution-processable complex. *Appl. Phys. Lett.,* 2009, **94**: Art. Nr. 041119.

[120] Lei K L, Chow C F, Tsang K C, Lei E N Y, Roy V A L, Lam M H W, Lee C S, Pun E Y B, Li J. Long aliphatic chain coated rare-earth nanocrystal as polymer-based optical waveguide amplifiers. *J. Mater. Chem.,* 2010, **20**: 7526.

[121] Wong W H, Pun E Y B, Chan K S. Er^{3+}-Yb^{3+} codoped polymeric optical waveguide amplifiers. *Appl. Phys. Lett.,* 2004, **84**: 176.

[122] Kahn A, Heinrich S, Kuhn H, Petermann K, Bradley J D B, Worhoff K, Pollnau M, Huber G. Low threshold monocrystalline Nd:$(Gd, Lu)_2O_3$ channel waveguide laser. *Optics Express,* 2009, **17**: 4412.

[123] Gaiduck M I, Grigoryants V V, Mironov A F, Roitman L D, Chissov V I, Rumiantseva V D, Sukhin G M. IR luminescence diagnostics of malignant-tumors with the help of metallocomplexes of porphyrins. *Dokl. Acad. Nauk. SSSR,* 1989, **309**: 980.

[124] Connally R E, Piper J A. Time-gated luminescence microscopy. *Ann. N. Y. Acad. Sci.,* 2008, **1130**: 106.

[125] New E J, Parker D, Smith D G, Walton J W. Development of responsive lanthanide probes for cellular applications. *Curr. Opin. Chem. Biol.,* 2010, **14**: 238.

[126] Ma Y, Wang Y. Recent advances in the sensitized luminescence of organic europium complexes. *Coord. Chem. Rev.,* 2010, **254**: 972.

[127] Allen K N, Imperiali B. Lanthanide-tagged proteins- an illuminating partnership. *Curr. Opin. Chem. Biol.,* 2010, **14**: 247.

[128] Allain C, Faulkner S. Photophysical approaches to responsive optical probes. *Future Medicinal Chemistry,* 2010, **2**: 339.

[129] Thibon A, Pierre V C. Principles of responsive lanthanide-based luminescent probes for cellular imaging. *Anal. Bioanal. Chem.,* 2009, **394**: 107.

[130] Petoud S. Novel antennae for luminescent lanthanide cations emitting in the visible and in the near-infrared: From small molecules to polymetallic lanthanide containing nanocrystals. *Chimia,* 2009, **63**: 745.

[131] Moore E G, Samuel A P S, Raymond K N. From antenna to assay: lessons learned in lanthanide luminescence. *Acc. Chem. Res.,* 2009, **42**: 542.

[132] Montgomery C P, Murray B S, New E J, Pal R, Parker D. Cell-penetrating metal complex optical probes: Targeted and responsive systems based on lanthanide luminescence. *Acc. Chem. Res.,* 2009, **42**: 925.

[133] Laurent S, Vander Elst L, Muller R N. Lanthanide complexes for magnetic resonance and optical molecular imaging. *Quart. J. Nucl. Med. Mol. Imag.,* 2009, **53:** 586.

[134] Degorce F, Card A, Soh S, Trinquet E, Knapik G P, Xie B. HTRF: a technology tailored for drug discovery - a review of theoretical aspects and recent applications. *Curr. Chem. Genom.,* 2009, **3**: 22.

[135] Bünzli J C G. Lanthanide luminescent bioprobes. *Chem. Lett.,* 2009, **38**: 104.

[136] Bazin H. Cryptates and their healthcare applications. *Actual. Chim.*, 2009, 20.

[137] Tsukube H, Noda Y, Shinoda S. Poly(arginine)-selective coprecipitation properties of self-assembling apoferritin and its Tb^{3+} complex: A new luminescent biotool for sensing of Poly(arginine) and its protein conjugates. *Chem. Eur. J.,* 2010, **16**: 4273.

[138] Berezin M Y, Achilefu S. Fluorescence lifetime measurements and biological imaging. *Chem. Rev.,* 2010, **110**: 2641.

[139] Andraud C, Maury O. Lanthanide complexes for nonlinear optics: From fundamental aspects to applications. *Eur. J. Inorg. Chem.,* 2009, **29-30**: 4357.

[140] He G S, Tan L S, Zheng Q, Prasad P N. Multiphoton absorbing materials: Molecular designs, characterizations, and applications. *Chem. Rev.,* 2008, **108**: 1245.

[141] Shao G S, Xue F M, Han R C, Tang M X, Wang Y A. Synthesis and characterization of europium complex nanoparticles with long-wavelength sensitized luminescence. *Acta Phys. Chim. Sin.,* 2010, **26**: 2031.

[142] Eliseeva S V, Auböck G, van Mourik F, Cannizo A, Song B, Deiters E, Chauvin A S, Chergui M, Bünzli J C G. Multiphoton-excited luminescent lanthanide bioprobes: two- and three-photon cross sections of dipicolinates derivatives and binuclear helicates. *J. Phys. Chem. B,* 2010, **114**: 2932.

[143] Alcala M A, Shade C M, Uh H, Gogick K, Modzelewski R A, Bartlett D L, Lee Y J, Petoud S, Brown C K. In vivo tumor targeting by functionalized dendrimer nanoscale complexes. *Ann. Surg. Oncol.,* 2010, **17**: S19.

[144] Shi M, Ding C R, Dong J W, Wang H Z, Tian Y P, Hu Z J. A novel europium(III) complex with versatility in excitation ranging from infrared to ultraviolet. *Phys. Chem. Chem. Phys.,* 2009, **11**: 5119.

[145] Soga K, Tokuzen K, Tsuji K, Yamano T, Hyodo H, Kishimoto H. NIR bioimaging: Development of liposome-encapsulated, rare-earth-doped Y_2O_3 nanoparticles as fluorescent probes. *Eur. J. Inorg. Chem.,* 2010, **2010**: 2673.

[146] Zhang P, Steelant W, Kumar M, Scholfield M. Versatile photosensitizers for photodynamic therapy at infrared excitation. *J. Am. Chem. Soc.*, 2007, **129**: 4526.

[147] Uh H, Badger P D, Geib S J, Petoud S. Synthesis and solid-state, solution, and luminescence properties of near-infrared-emitting neodymium(3+) complexes formed with ligands derived from salophen. *Helv. Chim. Acta,* 2009, **92**: 2313.

[148] Feng W, Sun L D, Zhang Y W, Yan C H. Synthesis and assembly of rare earth nanostructures directed by the principle of coordination chemistry in solution-based process. *Coord. Chem. Rev.,* 2010, **254**: 1038.

[149] Wang J A, Wang F, Xu J, Wang Y, Liu Y S, Chen X Y, Chen H Y, Liu X G. Lanthanide-doped $LiYF_4$ nanoparticles: Synthesis and multicolor upconversion tuning. *Comptes Rendus Chim.,* 2010, **13**: 731.

[150] Wu J, Tian Q, Hu H, Xia Q, Zou Y, Li F, Yi T, Huang C. Self-assembly of peptide-based multi-colour gels triggered by up-conversion rare earth nanoparticles. *Chem. Commun.,* 2009, (27): 4100.

[151] Shan J, Uddi M, Wei R, Yao N, Ju Y. The hidden effects of particle shape and criteria for evaluating the upconversion luminescence of the lanthanide doped nanophosphors. *J. Phys. Chem. C,* 2010, **114**: 2452.

[152] Wang F, Han Y, Lim C S, Lu Y H, Wang J, Xu J, Chen H Y, Zhang C, Hong M H, Liu X G. Simultaneous phase and size control of upconversion nanocrystals through lanthanide doping. *Nature,* 2010, **463**: 1061.

[153] Feng J, Song S Y, Deng R P, Fan W Q, Zhang H J. Novel multifunctional nanocomposites: Magnetic mesoporous silica nanospheres covalently bonded with near-infrared luminescent lanthanide complexes. *Langmuir,* 2010, **26**: 3596.

[154] Das G K, Heng B C, Ng S C, White T, Loo J S C, D'Silva L, Padmanabhan P, Bhakoo K K, Selvan S T, Tan T T Y. Gadolinium oxide ultranarrow nanorods as multimodal contrast agents for optical and magnetic resonance imaging. *Langmuir,* 2010, **26**: 8959.

[155] Shen J, Sun L D, Zhang Y W, Yan C H. Superparamagnetic and upconversion emitting Fe_3O_4/$NaYF_4$:Yb,Er heteronanoparticles via a crosslinker anchoring strategy. *Chem. Commun.,* 2010, **46**: 5731.

[156] Sun L D, Gu J Q, Zhang S Z, Zhang Y W, Yan C H. Luminescence resonance energy transfer based on beta-$NaYF_4$:Yb, Er nanoparticles and TRITC dye. *Sci. China. Ser. B-Chem.,* 2009, **52**: 1590.

[157] Bednarkiewicz A, Nyk M, Samoc M, Strek W. Up-conversion FRET from Er^{3+}/Yb^{3+}:$NaYF_4$ nanophosphor to CdSe quantum dots. *J. Phys. Chem. C,* 2010, **114**: 17535.

[158] Wang L, Zhang Y, Zhu Y. One-pot synthesis and strong near-infrared upconversion luminescence of poly(acrylic acid)-functionalized YF_3:Yb^{3+}/Er^{3+} nanocrystals. *Nano Res.,* 2010, **3**: 317.

[159] Li D, Dong B, Bai X, Wang Y, Song H. Influence of the TGA modification on upconversion luminescence of hexagonal-phase $NaYF_4$:Yb^{3+}, Er^{3+} nanoparticles. *J. Phys. Chem. C,* 2010, **114**: 8219.

[160] Kobayashi H, Ogawa M, Alford R, Choyke P L, Urano Y. New strategies for fluorescent probe design in medical diagnostic imaging. *Chem. Rev.,* 2010, **110**: 2620.

[161] Xiong L, Yang T, Yang Y, Xu C, Li F. Long-term in vivo biodistribution imaging and toxicity of polyacrylic acid-coated upconversion nanophosphors. *Biomaterials,* 2010, **31**: 7078.

[162] Kobayashi H, Kosaka N, Ogawa M, Morgan N Y, Smith P D, Murray C B, Ye X C, Collins J, Kumar G A, Bell H, Choyke P L. In vivo multiple color lymphatic imaging using upconverting nanocrystals. *J. Mater. Chem.,* 2009, **19**: 6481.

[163] Wang M, Mi C, Zhang Y, Liu J, Li F, Mao C, Xu S. NIR-responsive silica-coated $NaYbF_4$:Er/Tm/Ho upconversion fluorescent nanoparticles with tunable emission colors and their applications in immunolabeling and fluorescent imaging of cancer cells. *J. Phys. Chem. C,* 2009, **113**: 19021.

[164] Wu S W, Han G, Milliron D J, Aloni S, Altoe V, Talapin D V, Cohen B E, Schuck P J. Non-blinking and photostable upconverted luminescence from single lanthanide-doped nanocrystals. *Proc. Ntl. Acad. Sci. USA,* 2009, **106**: 10917.

[165] Babu S, Cho J H, Dowding J M, Heckert E, Komanski C, Das S, Colon J, Baker C H, Bass M, Self W T, Seal S. Multicolored redox active upconverter cerium oxide nanoparticle for bio-imaging and therapeutics. *Chem. Commun.,* 2010, **46**: 6915.

[166] Fernandez-Moreira V, Song B, Sivagnanam V, Chauvin A S, Vandevyver C D B, Gijs M A M, Hemmilä I A, Lehr H A, Bünzli J C G. Bioconjugated lanthanide luminescent helicates as multilabels for lab-on-a-chip detection of cancer biomarkers. *Analyst,* 2010, **135**: 42.

[167] Ma Q, Su X. Near-infrared quantum dots: synthesis, functionalization and analytical applications. *Analyst,* 2010, **135**: 1867.

[168] Cheng L, Yang K, Zhang S, Shao M, Lee S, Liu Z. Highly-sensitive multiplexed in vivo imaging using pegylated upconversion nanoparticles. *Nano Res.,* 2010, **3**: 722.

[169] Richards B S. Enhancing the performance of silicon solar cells via the application of passive luminescence conversion layers. *Solar En. Mat. Sol. Cells,* 2006, **90**: 2329.

[170] Kalyanasundaram K. Dye-sensitized Solar Cells. Lausanne: EPFL Press, 2010.

[171] Dexter D L. Two ideas on energy transfer phenomena: ion-pair effects involving the OH stretching mode and sensitization of photovoltaic cells. *J. Lumin.,* 1979, **18**: 779.

[172] Munz P, Bucher E. The use of rare earths in photovoltaics. *The Rare Earths in Modern Science and Technology,* 1982, **3**: 547.

[173] Reisfeld R. Future technological applications of rare earth doped materials. *J. Less-Common Met.,* 1983, **93**: 243.

[174] Reisfeld R. Industrial applications of rare earths in fiber optics, luminescent solar concentrators and lasers. *Inorg. Chim. Acta,* 1987, **140**: 345.

[175] Jin T, Inoue S, Machida K, Adachi G. Photovoltaic cell characteristics of hybrid silicon devices with lanthanide complex phosphor-coating film. *J. Electrochem. Soc.,* 1997, **144**: 4054.

[176] Kawano K, Arai K, Yamada H, Hashimoto N, Nakata R. Ap-

plication of rare-earth complexes for photovoltaic precursors. *Solar En. Mat. Sol. Cells,* 1997, **48**: 35.

[177] Marchionna S, Meinardi F, Acciarri M, Binetti S, Papagni A, Pizzini S, Malatesta V, Tubino R. Photovoltaic quantum efficiency enhancement by light harvesting of organo-lanthanide complexes. *J. Lumin.,* 2006, **118**: 325.

[178] Chen D Q, Wang Y S, Yu Y L, Huang P, Weng F Y. Near-infrared quantum cutting in transparent nanostructured glass ceramics. *Opt. Lett.,* 2008, **33**: 1884.

[179] Trupke T, Green M A, Wurfel P. Improving solar cell efficiencies by down-conversion of high-energy photons. *J. Appl. Phys.,* 2002, **92**: 1668.

[180] Richards B S. Luminescent layers for enhanced silicon solar cell performance: Down-conversion. *Solar En. Mat. Sol. Cells,* 2006, **90**: 1189.

[181] van Wijngaarden J T, Scheidelaar S, Vlugt T J H, Reid M F, Meijerink A. Energy transfer mechanism for downconversion in the (Pr^{3+}, Yb^{3+}) couple. *Physical Review B,* 2010, **81**: Art. Nr. 155112.

[182] Meijer J M, Aarts L, van der Ende B M, Vlugt T J H, Meijerink A. Downconversion for solar cells in YF_3:Nd^{3+}, Yb^{3+}. *Phys. Rev. B,* 2010, **81**: Art. Nr. 035107.

[183] Eilers J J, van Wijngaarden J T, Krämer K, Güdel H U, Meijerink A. Efficient visible to infrared quantum cutting through downconversion with the Er^{3+}–Yb^{3+} couple in $Cs_3Y_2Br_9$. *Appl. Phys. Lett.,* 2010, **96**: Art. Nr. 151106.

[184] van der Ende B M, Aarts L, Meijerink A. Near-infrared quantum cutting for photovoltaics. *Adv. Mater.,* 2009, **21**: 3073.

[185] Richards B S, Shalav A. Enhancing the near-infrared spectral response of silicon optoelectronic devices via up-conversion. *IEEE Trans. Electron. Dev.,* 2007, **54**: 2679.

[186] Ivanova S, Pelle F. Strong 1.53 μm to NIR-VIS-UV upconversion in Er-doped fluoride glass for high-efficiency solar cells. *J. Opt. Soc. Am. B: Opt. Phys.,* 2009, **26**: 1930.

[187] Liao M, Qin G, Yan X, Hughes M, Suzuki T, Ohishi Y. Evaluating upconversion materials developed to improve the efficiency of solar cells: comment. *J. Opt. Soc. Am. B,* 2010, **27**: 1352.

[188] Shpaisman H, Niitsoo O, Lubomirsky I, Cahen D. Can up- and down-conversion and multi-exciton generation improve photovoltaics. *Solar En. Mat. Sol. Cells,* 2008, **92**: 1541.

[189] Grätzel M. Solar Energy conversion by dye-sensitized photovoltaic cells. *Inorg. Chem.,* 2005, **44**: 6841.

[190] Wang Q, Li Y, Yan X Z, Rathi M, Ropp M, Galipeau D, Jiang J Z. Organic photovoltaic cells made from sandwich-type rare earth phthalocyaninato double and triple deckers. *Appl. Phys. Lett.,* 2008, **93**: Art. Nr. 073303.

[191] Oh J H, Song H M, Kim H K. Abstracts, First International Conference on Luminescence of Lanthanides, Odessa, Ukraine, Sept.5–9, 2010, 88.

[192] Service R F. Nations move to head off shortages of rare earths. *Science,* 2010, **327**: 1596.

[193] Currie M J, Mapel J K, Heidel T D, Goffri S, Baldo M A. High-efficiency organic solar concentrators for photovoltaics. *Science,* 2008, **321**: 226.

[194] Zhou J, Sun Y, Du X, Xiong L, Hu H, Li F. Dual-modality in vivo imaging using rare-earth nanocrystals with near-infrared to near-infrared (NIR-to-NIR) upconversion luminescence and magnetic resonance properties. *Biomaterials,* 2010, **31:** 3287.

[195] Zhang C, Sun L D, Zhang Y W, Yan C H. Rare earth upconversion nanophosphors: synthesis, functionalization and application as biolabels and energy transfer donors. *J. Rare Earth*s, 2010, **28**(6): 807.